EurJOC European Journal of Organic Chemistry

FULL PAPER

Pyrazine Fluorophores

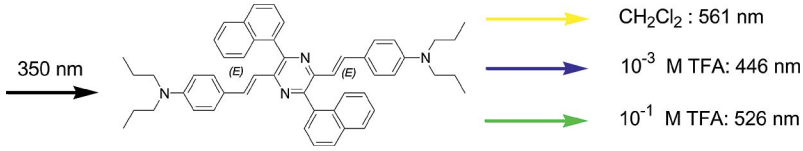

Centrosymmetric diaryldistyrylpyrazines with terminal acceptor and donor groups have been prepared. The electronic spectra are highly sensitive towards changes in the environment: solvatochromism and huge Stokes shifts result from large dipole moments of the C_2-symmetric dyes. Protonation induces multiple alterations of absorption and emission, thus allowing optical sensing of the pH and polarity.

Keywords: Solvatochromism / Acidochromism / Fluorescence / Nitrogen heterocycles / Conjugation

DOI: 10.1002/ejoc.201300463

Diaryldistyrylpyrazines: Solvatochromic and Acidochromic Fluorophores

Volker Schmitt,[a] Sebastian Moschel,[a] and Heiner Detert*[a]

Dedicated to Professor Wolfgang Liptay on the occasion of his 85th birthday

Keywords: Solvatochromism / Acidochromism / Fluorescence / Nitrogen heterocycles / Conjugation

Diaryldimethylpyrazines are the starting materials for the synthesis of C_2-symmetric donor- or acceptor-substituted distyrylpyrazines. The optical properties of these cruciform-shaped dyes are dominated by the distyrylpyrazine units; the photophysics is controlled by the styryl substitution, the diaryl substituents on the central pyrazine only having a small effect. Protonation occurs on the pyrazine and/or lateral amines or azines, thereby altering the absorption and emission properties. Hypso- and bathochromism as well as fluorescence quenching depend on the nature of the terminal substituent. This, and a significant positive solvatochromism of the fluorescence, allow optical sensing of the pH and polarity of the environment.

Introduction

Organic semiconductors of the distyrylbenzene type (DSB) have great potential as active materials in optoelectronic devices,[1] as nonlinear optical materials,[2] and as sensors.[3] Two strategies have been successfully applied to adjust the (nonlinear) optical and electronic properties of the fundamental chromophore. Although the extension of the conjugated system is of limited effect,[4] substitution with electron-pair donating (EPD) and/or withdrawing (EPA) groups[5] allows marked alterations of the absorption and fluorescence maxima, quantum yield, two-photon cross-section, ionization potential, and electron affinity. Furthermore, the substituents can be designed to allow interaction with external stimuli.[6] Electronic coupling between these EPA/EPD groups and the π system can result in optical responses like shifts of absorption and emission maxima or fluorescence quantum yields.

The optical sensing of polarity, ions, pH, and other solutes with fluorescent dyes has become an important tool for the analysis of local properties and in imaging.[7] Applications range from the fuel industry to the investigation of biological tissues.[8] Fluorescent probes can be used in solution[7c] or, immobilized in polymeric matrices,[7a,8a] in flow cells. Dyes with an emission above 550 nm are preferred for biological sensing because they do not interfere with the autofluorescence of tissues. Furthermore, the enhanced optical transparency of tissues from 650 to 900 nm allows excitation of the fluorescent probe by two-photon absorption.[9]

The replacement of a benzene ring in a DSB by pyridine or related azines results, as an EPA substituent, in enhanced electron affinity.[10] Because these rings can act as bases or ligands, they provide a further pathway to influence optical properties.[11] Similarly, amines act as bases and acceptors for hydrogen bridging. Whereas the protonation or quaternization of amines changes their character from donor to acceptor, the acceptor strength of pyridine and related moieties is greatly enhanced upon protonation or quaternization.[12] Complexation with Lewis acids or protonation has been shown to cause significant changes in the electronic spectra of π-conjugated chromophores with basic sites at terminal positions.[11] As triarylamines are very poor bases they are protonated only under extreme forcing conditions, thus preserving their electron-donating effect even in the presence of strong acids.

As part of our interest in fluorophores with switchable optical properties and efficient two-photon absorption,[2b,5] we report herein the synthesis of C_2-symmetrical 2,5-distyrylpyrazines (DSPs) with central diaryl substitution. A few donor-substituted distyrylpyrazines are known,[13] and some of their photophysical[14] and solid-state properties[15] have been studied. The generally applied synthetic routes to styrylpyrazines are based on the Lewis acid catalyzed condensation of aromatic aldehydes[16] and on the deprotonation of methylpyrazines and aldol condensation with aromatic aldehydes. Variations like the Siegrist reaction[17] or phase-transfer conditions[18] proved to be advantageous in specific preparations.

In these DSP chromophores, pyrazine acts as an electron acceptor resulting in a donor–acceptor–donor electronic

[a] Institute for Organic Chemistry, Johannes Gutenberg-University Mainz,
Duesbergweg 10–14, 55099 Mainz, Germany
E-mail: detert@uni-mainz.de
Homepage: http://www.blogs.uni-mainz.de/fb09ak-detert/

Supporting information for this article is available on the WWW under http://dx.doi.org/10.1002/ejoc.201300463.

structure. The internal charge transfer depends on the relative strength of the EPA/EPD substituents and is tuned by external stimuli. To study the impact of polar and protic environments on the electronic transitions, the substitution on the termini has been systematically varied from (basic) acceptor to basic and nonbasic donor as has the donor substitution on the central diphenylpyrazine unit. Interactions of these di- or multipolar compounds with the environment can result in optical responses that are useful for sensing purposes.[19]

Results

Synthesis

The general strategy for the construction of centrosymmetric diaryldistyrylpyrazines **1**–**12** started with the synthesis of 2,5-dimethylpyrazines **17** with appropriate 3,6-diaryl substitution. A base-induced condensation of the methyl groups with suitable benzaldehydes **18** yielded the title compounds. For the synthesis of dimethyldiarylpyrazines **17**, ethyl acetoacetate was first nitrosated in aqueous solution. A copper-catalyzed Sandmeyer-like coupling with diazotized anilines yielded the 1-aryl-substituted hydroxyiminoacetones **14a**–**c** (Scheme 1). These compounds can also be prepared by nitrosation of arylacetones **13a**,**b**,**d** in nonaqueous solution. Reduction of the hydroxyimino ketones **14** in alkaline solution led to the 2,5-diaryl-substituted heterocycles **16** by condensation of the initially formed amino ketones **15**. Aromatization to **17** was achieved by the oxidation of the dihydropyrazines **16** with air in moderate yields. Pyrazine **17e** with terminal carbazole units was obtained in 80% yield by Ullmann condensation of the bromo compound **17b** with carbazole.

A variety of base/solvent systems were studied for the two-fold base-induced condensation of the dimethylpyrazines **17** with benzaldehydes **18**; the best results were obtained with potassium *tert*-butoxide in DMF. Nevertheless, even under these optimized conditions, the yields of the desired DSPs **1**–**10** varied from poor to good (19–78%; Scheme 2, Table 1). No DSP was obtained in the reactions with the electron-deficient *p*-cyanobenzaldehyde. Oxidation of the dimethylpyrazines **17a**,**c** with SeO_2 led to the corresponding pyrazinedicarbaldehydes **19a**,**c** (56%) and subsequent two-fold Horner olefination allowed the direct condensation to be bypassed resulting in DSPs **2**, **11**, and **12** with cyano- and α-quinolyl end-groups.

Structures of Distyrylpyrazines

The structures **1**–**12** were determined by spectroscopic methods, including 2D NMR spectroscopy. After chromatography and recrystallization, all the compounds were isolated as (*E*,*E*)-DSPs without detectable traces of other isomers.

Single crystals of compound **5** were obtained by slow evaporation of a solution of dichloromethane/methanol. In contrast to the centrosymmetry of the molecular structure in solution, the molecule adopts a noncentrosymmetric conformation in the crystal (Figure 1). Steric crowding due to four substituents on the pyrazine results in large dihedral angles of –129.2° (N1–C2–C7–C8) and –131.4° (N4–C5–C13–C18) in the teraryl axis. These distortions are slightly larger than those reported for tetraphenylpyrazine (41.1 and 48.8°).[20] Compared with the terphenyl axis, the distyrylpyrazine system is more planar. Nevertheless, the dihedral angles between the pyrazine and vinylene moieties of –164.5° (C2–C3–C19–C20) and –175.3° (C5–C6–C34–C35) and those between the vinylene and aniline ring of –162.8° (C19–C20–C21–C26) and –171.8° (C34–C35–C36–C37) are significantly larger than those found in a similar compound with central 3,6-dimethyl (<3.5°) or distyryl substitution (0.3°).[21] The sums of angles around the aniline N atoms of 358.8° (N27) and 359.5° (N42), the dihedral angles between the dialkylamino groups and benzene rings of nearly 179° (C40–C39–N42–C43: –173.8°; C25–C24–N27–C28: 173.9), and the short aniline C–N bonds of 1.381 Å (C39–N42) and 1.377 Å (C24–N27) indicate a strong electronic coupling between the peripheral donor groups and the cen-

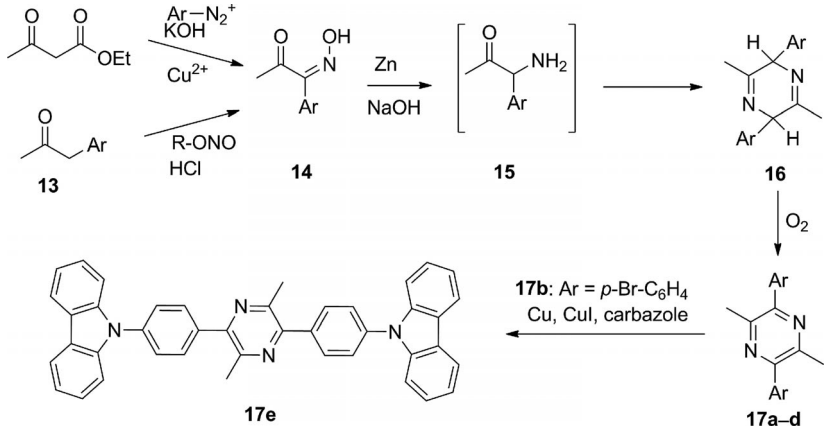

Scheme 1. Synthesis of 2,5-dimethyl-3,6-diarylpyrazines **17**. **a**: Ar = phenyl; **b**: Ar = 4-bromophenyl; **c**: Ar = 4-methoxyphenyl; **d**: Ar = 1-naphthyl.

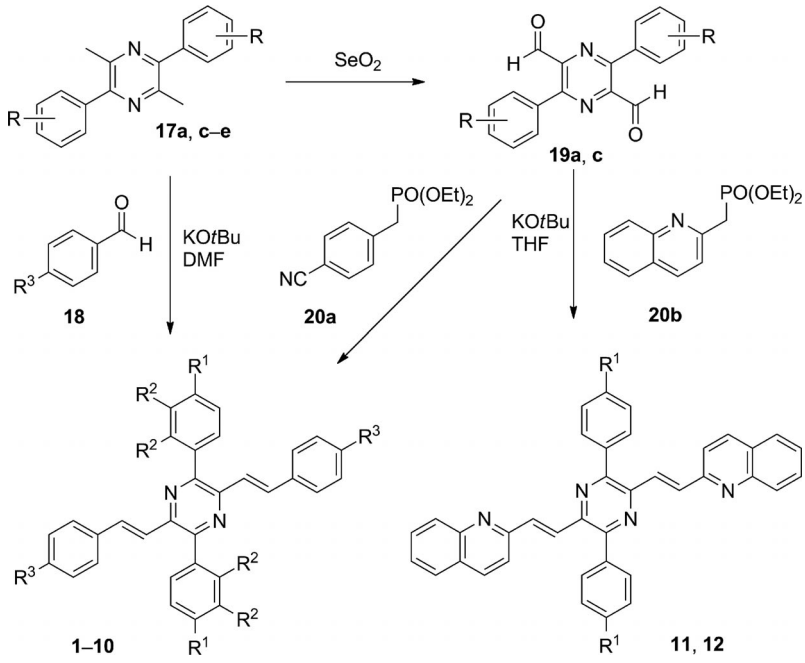

Scheme 2. Synthesis of 2,5-distyryl-3,6-diarylpyrazines **1**–**12**.

Table 1. Substitution pattern of DSPs **1**–**12**.

	R^1	R^2	R^3	Yield [%]	Color
1	H	H	H	64	yellow
2	H	H	CN	71	yellow
3	H	H	OC_8H_{17}	67	yellow
4	H	H	9-Carbaz.[a]	32	yellow
5	H	H	$N(C_3H_7)_2$	57	orange
6	H	H	*N*-Crown[b]	19	red
7	H	naphth.[c]	OC_6H_{13}	29	yellow
8	H	naphth.[c]	$N(C_3H_7)_2$	21	orange
9	OCH_3	H	$N(C_3H_7)_2$	39	red
10	9-Carbaz.	H	$N(CH_3)_2$	78	orange
11	H	H		48	orange
12	OCH_3	H		85	yellow

[a] 9-carbaz. = 9-carbazolyl. [b] *N*-crown = 1,4,7,10-tetraoxa-13-aza-13-cyclopentadecyl. [c] Phenyl replaced by α-naphthyl.

tral pyrazine. All the structural information indicates that the main conjugation path extends along the bis(aminostyryl)pyrazine axis.

Optical Properties

The fluorophores **1**–**12** form yellow, orange, or red solids, and also colored and fluorescent solutions. Increasing donor strength correlates with a more intense color in solution. Diphenyldistyrylpyrazine **1** represents the fundamental chromophore of the series **1**–**12**. In cyclohexane, the long-wavelength absorption band of **1** peaks at λ_{max} = 398 nm and emission occurs at λ^F_{max} = 442 nm. A comparison of the optical data of **1** with those of simple 2,5-distyrylpyrazine lacking the diphenyl substitution (λ_{max} =

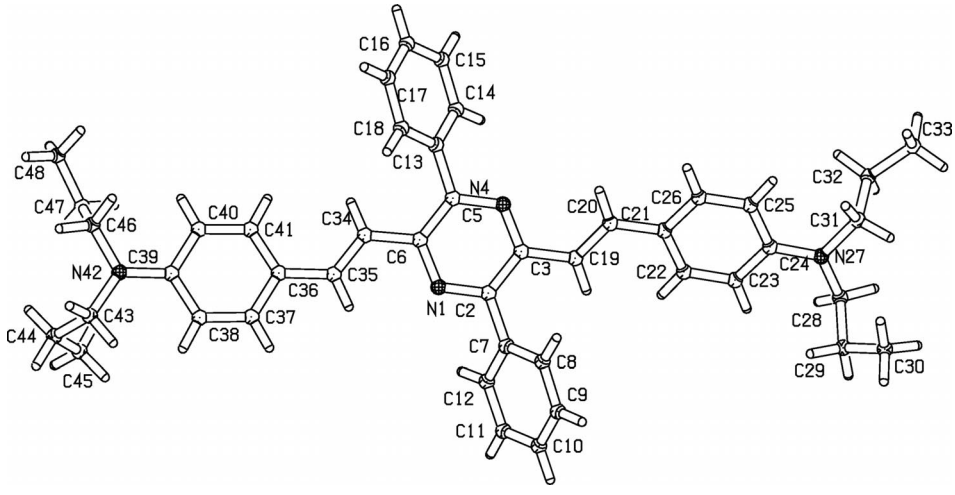

Figure 1. Molecular structure of **5**.

382 nm, λ^{F}_{max} = 424 nm in cyclohexane[14e]) reveals a significant influence of these phenyl rings: Both transitions in **1** are redshifted by about 17 nm ($\Delta\tilde{\nu}^{Abs}$ = 1052 cm^{-1}, $\Delta\tilde{\nu}^{F}$ = 960 cm^{-1}; Table 2).

Table 2. Optical properties and solvatochromism of **1**–**12**.

Comp.: λ [nm] Φ	CH	Tol	DCM	AN	EtOH	log ε_{max} [M^{-1} cm^{-1}] in DCM
1: λ_{max}	398	402	401	397	398	4.58
λ^{F}_{max}	442	447	452	450	453	
Φ	0.02	0.03	0.02	0.005	0.02	
2: λ_{max}	403	408	406	402	402	4.64
λ^{F}_{max}	453	454	459	460	458	
Φ	0.05	0.07	0.06	0.04	0.05	
3: λ_{max}	413	419	418	414	414	4.63
λ^{F}_{max}	456	466	477	479	494	
Φ	0.16	0.19	0.15	0.09	0.13	
4: λ_{max}	416	422	419	414	412	4.79
λ^{F}_{max}	463	475	490	502	493	
Φ	0.24	0.31	0.26	0.05	0.02	
5: λ_{max}	456	468	479	477	474	4.82
λ^{F}_{max}	502	524	561	570	584	
Φ	0.34	0.25	0.11	0.11	0.09	
6: λ_{max}	455	466	470	468	467	4.78
λ^{F}_{max}	501	522	536	561	574	
Φ	0.19	0.22	0.29	0.17	0.10	
7: λ_{max}	413	419	417	412	414	4.57
λ^{F}_{max}	453	464	474	475	492	
Φ	0.10	0.15	0.13	0.08	0.08	
8: λ_{max}	459	474	486	484	486	4.73
λ^{F}_{max}	505	526	561	575	583	
Φ	0.13	0.11	0.06	0.03	0.03	
9: λ_{max}	455	468	477	475	474	4.49
λ^{F}_{max}	502	523	556	566	584	
Φ	0.12	0.14	0.08	0.06	0.04	
10: λ_{max}	452	467	471	466	464	4.76
λ^{F}_{max}	505	527	554	571	580	
Φ	0.28	0.27	0.17	0.12	0.08	
11: λ_{max}	408	412	411	407	407	4.76
λ^{F}_{max}	456	463	463	464	463	
Φ	0.03	0.06	0.06	0.02	0.04	
12: λ_{max}	421	426	423	421	422	4.80
λ^{F}_{max}	479	492	493	491	497	
Φ	0.08	0.17	0.16	0.13	0.16	

Symmetrical substitution by cyano groups (**2**) causes weak redshifts of absorption ($\Delta\lambda$ = 5 nm, $\Delta\tilde{\nu}^{Abs}$ = 250 cm^{-1}) and fluorescence maxima ($\Delta\lambda$ = 11 nm, $\Delta\tilde{\nu}^{F}$ = 549 cm^{-1}), and the larger π system of the α-quinolyl moiety (**11**) results in a slightly greater shift. Groups with a moderate electron-donating effect (**3**: *O*-hexyl; **4**: *N*-carbazolyl) on the styryl units shift the absorption and fluorescence maxima by 15–25 nm ($\Delta\tilde{\nu}^{F}$ = 695–1087 cm^{-1}) to the red, but with the stronger dialkylamino donors (**5** and **6**), the displacements in cyclohexane are about three times larger (λ_{max} = 456/455 nm, $\Delta\lambda$ = 58/57 nm, $\Delta\tilde{\nu}^{Abs}$ = 3196/3148 cm^{-1}; λ^{F}_{max} = 502/501 nm, $\Delta\lambda^{F}$ = 60/59 nm, $\Delta\tilde{\nu}^{F}$ = 2704/2664 cm^{-1}). Increasing the size of the central aryl moieties from a phenyl substituent (**3** and **5**) to the sterically more demanding α-naphthyl group (**7** and **8**) or to phenyl groups bearing electron-donating groups (**9** and **10**) has only a negligible effect on the position of the maxima in the electronic spectra ($\Delta\lambda \leq$ 4 nm). This is valid as long as the DSP unit carries donor substituents. DSPs **11** and **12** composed of electron-deficient quinoline and pyrazine units show that methoxy donors on the central teraryl axis have a significant effect on the spectra. Whereas the electronic transitions of **11** occur at λ_{max} = 408 nm and λ^{F}_{max} = 456 nm, methoxy substitution on the teraryl axis (**12**) shifts these maxima by about $\Delta\lambda_{max}$ = 13 nm ($\Delta\tilde{\nu}^{Abs}$ = 757 cm^{-1}) and $\Delta\lambda^{F}_{max}$ = 23 nm ($\Delta\tilde{\nu}^{F}$ = 1053 cm^{-1}) to lower energies.

The fluorescence quantum yields of DSPs **1**, **2**, and **11** without donor substitution are low (Φ = 0.02–0.05 in cyclohexane), but even weak donor groups significantly enhance the quantum yield (Φ = 0.08–0.16 for **3**, **7** and **12** in cyclohexane). With Φ = 0.24–0.34, amino-substituted DSPs **4**, **5**, and **10** are the most efficient emitters.

Semi-empirical calculations at the INDO/S level[22] gave absorption bands with significantly higher energies. But the correlation of substituent effects within the experimental data and within the theoretical data is striking: Although diphenyl substitution on the pyrazine ring of distyrylpyrazine causes a redshift (exp./calcd.: $\Delta\lambda$ = 16/24 nm), the position of the absorption maximum is independent of central phenyl (**3**) or naphthyl (**7**) substitution, whereas exchange of the central naphthyl groups in **8** by *p*-anisyl (**9**) causes a blueshift (exp./calcd.: $\Delta\lambda$ = –7/–4 nm).

Solvatochromism

Solvatochromism of the fundamental chromophore **1** as well as of **2** and **11** is very weak, both in absorption and emission. The effect of electron-pair donating groups of moderate strength on the solvatochromic displacement of the absorption maxima of **3** and **4** is small, but their fluorescence is more sensitive: Positive solvatochromism shifts the emission to the red ($\Delta\lambda^{F}_{max}$ = 38 and 30 nm, $\Delta\tilde{\nu}^{F}$ = 1687 and 1314 cm^{-1}, for cyclohexane and ethanol, respectively). With strong donors on the terminal rings (**5**, **6**, **8**–**10**) a remarkable increase in the solvatochromic sensitivity can be noted: Displacements of $\Delta\lambda$ = 12–19 nm ($\Delta\tilde{\nu}$ = 572–881 cm^{-1}) in absorption and of $\Delta\lambda$ = 73–82 nm ($\Delta\tilde{\nu}$ = 2538–2797 cm^{-1}) in emission separated the maxima recorded in cyclohexane from those in ethanol (Table 2, Figure 2).

Replacing the central phenyl rings by α-naphthyl groups (**3**, **5** and **7**, **8**) or by donor-substituted anisyl rings (**5**, **9** and **11**, **12**) only slightly modifies the solvatochromic characteristics. The fluorescence efficiencies of **1**–**12** are higher in solvents of low polarity like cyclohexane and toluene. The fluorescence efficiencies are reduced with increasing polarity. This sensitivity is poor for DSPs with terminal acceptors (**1**, **2**, **11**, **12**: ca. 75–90%). Dyes **3** and **7** with alkoxy donors are less emissive in highly polar solvents (ca. 50%) and the residual fluorescence of amino-substituted DSPs **4**–**6** and **8**–**10** in ethanol or acetonitrile drops to values of 15–30%.

Acidochromism

Due to the nitrogen atoms in the central ring, distyrylpyrazine **1** is a weak base. Addition of TFA to solutions of **1** in dichloromethane results in the protonation of **1**. In

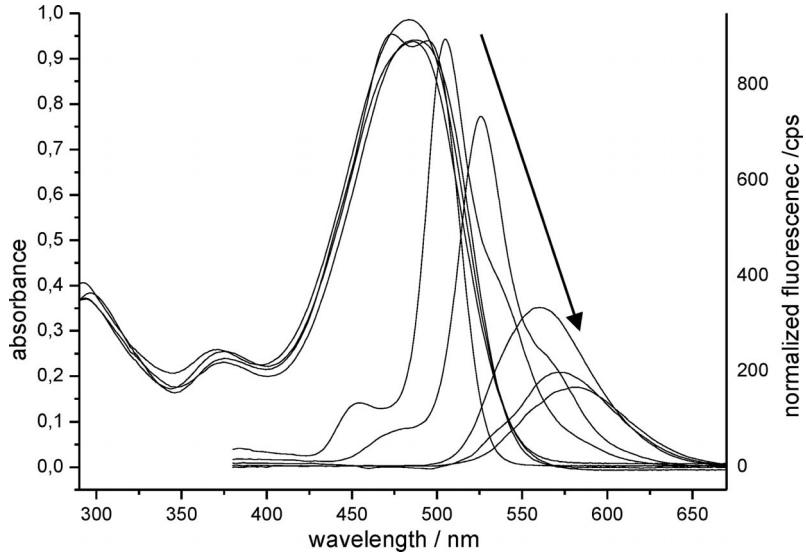

Figure 2. Electronic spectra of **8** in different solvents (fluorescence normalized to identical optical density at λ^{exc} = 345 nm; cps = counts s^{-1}).

10^{-2} M TFA, the UV/Vis spectrum is nearly a 1:1 superposition of the spectra of neutral **1** and **1** + H^+; in 0.1 M TFA only **1** + H^+ is visible, as indicated by a significant redshift to λ_{max} = 470 nm ($\Delta\lambda$ = 69 nm, $\Delta\tilde{\nu}$ = 3661 cm^{-1}; Table 3). The impact of acid on the fluorescence is similar. In 10^{-2} M TFA the spectrum is composed of emission mainly from **1** + H^+ together with the residual emission from **1**; in 0.1 M TFA the fluorescence peaks at 578 nm, a redshift of about 126 nm ($\Delta\tilde{\nu}$ = 4823 cm^{-1}) compared with the emission of the neutral form. Higher concentrations of TFA (1 M) provoke further shifts of the absorption up to λ = 484 nm ($\Delta\tilde{\nu}$ = 615 cm^{-1}) and the emission shifts to λ^F = 579 nm. Protonation results in a reduced extinction coefficient (ca. 50%) and fluorescence efficiency (ca. 30%). The cyano groups in **2** reduce the basicity. For both, absorption and emission, 1 M TFA was needed to observe protonated **2**, and the bathochromic shifts are very small ($\Delta\lambda$ = 10 nm, $\Delta\lambda^F$ = 34 nm; $\Delta\tilde{\nu}^{Abs}$ = 592 cm^{-1}, $\Delta\tilde{\nu}^F$ = 1503 cm^{-1}). The basicity of the pyrazine is weakly affected by alkoxy donors (**3**, **7**). TFA (10^{-2}–10^{-1} M) shifts the absorption maxima to the red ($\Delta\lambda$ = 126–137 nm, $\Delta\tilde{\nu}$ = 5541–5930 cm^{-1}) and, because protonated **3** and **7** are not emissive, quenches the fluorescence. The relative sensitivity of their absorption spectra towards TFA is **3** < **1** < **7**.

Like the absorption maxima, the fluorescence quantum yields are dependent on the concentration of TFA. The impact of TFA is small for **1**, **2**, and **11** without donor groups, but the quantum yields of DSPs **4** and **7** with terminal donor groups are reduced with increasing TFA concentration, with 1 M TFA totally quenching the emission. On the other hand, the protonation of the terminal amino groups in **5**, **6**, and **9** results first in a decrease in the quantum yield of the emission of the neutral compound followed by the appearance of a strongly emissive protonated species (Φ = 0.2–0.4). Even the second protonated species exhibit significant fluorescence quantum yields (Φ = 0.14–0.25).

Uniquely, 1 M TFA is required to protonate the carbazole analogue **4**, with only traces of protonated **4** visible in 0.1 M TFA. The fluorescence is more sensitive: The efficiency of the emission of **4** in 0.1 M TFA is reduced to 30%, and protonated **4** is not fluorescent. In contrast to **4**, the nitrogen atoms in the terminal quinolines in DSP **11** are basic sites and **11** shows two distinct species (Figure 3). Protonation starts in 10^{-4} M TFA and is complete in 10^{-2} M TFA. The absorption maxima are separated by $\Delta\lambda$ = 43 nm ($\Delta\tilde{\nu}^{Abs}$ = 2304 cm^{-1}) and the spectra show an isosbestic point at λ = 430 nm. A second protonation in 1 M TFA causes a weak blueshift and hypsochromism. In the emission spectra an isostilbic point (λ = 504 nm) was observed in the transformation of neutral (λ^F_{max} = 463 nm) to protonated **11** (λ^F_{max} = 531 nm, $\Delta\tilde{\nu}^F$ = 2766 cm^{-1}). In 10^{-4} M TFA, a nearly equimolar equilibrium of both species is observed. The spectra show that a second protonated form of excited **11** appears in 1 M TFA with an emission maximum (λ^F_{max} = 476 nm, $\Delta\tilde{\nu}$ = ^{F} = 590 cm^{-1}) close to that of the neutral molecule (Figure 3). The methoxy derivative **12** shows slightly enhanced basicity and similar effects of TFA on the absorption, but the fluorescence behavior is completely different. In 10^{-3} M TFA, the emission of the neutral form has vanished in favor of a weak band at around λ^F = 600 nm ($\Delta\tilde{\nu}^F$ = 3836 cm^{-1}) that decreases at higher concentrations.

Contrary to the protonation-induced bathochromism of the absorption and emission of the dyes **1**–**4** and **7**, those with dialkylaminostyryl groups (**5**, **6**, **8**–**10**) are more easily protonated, with the absorption and emission spectra of the protonated dyes exhibiting peaks at shorter wavelengths.

Table 3. Acidochromism of **1**–**12** in dichloromethane/TFA.

Comp.: λ [nm]	TFA [M]						
Φ	DCM	10^{-5}	10^{-4}	10^{-3}	10^{-2}	10^{-1}	1
1: λ_{max}	401	401	401	401	416	470	484
λ^{F}_{max}	452	452	452	452	569	578	579
Φ	0.02	0.02	0.02	0.02	0.015	0.01	0.005
2: λ_{max}	406	406	406	406	406	406	416
λ^{F}_{max}	459	459	459	459	459	459	493
Φ	0.05	0.04	0.04	0.04	0.04	0.04	0.05
3: λ_{max}	418	418	418	418	418	513	544
λ^{F}_{max}	477	478	478	478	478	479	–
Φ	0.16	0.17	0.16	0.16	0.72	0.11	0
4: λ_{max}	419	419	419	419	419	419	549
λ^{F}_{max}	490	491	492	493	493	493	–
Φ	0.24	0.25	0.24	0.25	0.24	0.08	0
5: λ_{max}	479	479	479	473	399	398	411
λ^{F}_{max}	561	561	562	576	443	453	482
Φ	0.11	0.11	0.10	0.05	0.20	0.22	0.25
6: λ_{max}	470	470	466	398	396	422	425
λ^{F}_{max}	536	589	450/589	439	455	514	517
Φ	0.29	0.15	0.15	0.05	0.21	0.19	0.14
7: λ_{max}	417	417	417	417	519	534	554
λ^{F}_{max}	474	474	474	474	476	–	–
Φ	0.13	0.10	0.11	0.10	0.02	0	0
8: λ_{max}	486	486	477	395	393	435	442
λ^{F}_{max}	561	561	583/446	446	442	528	532
Φ	0.06	0.05	0.03	0.05	0.04	0.02	0.01
9: λ_{max}	477	477	477	472	414	413	454
λ^{F}_{max}	556	556	557	574	472	481	524
Φ	0.12	0.12	0.12	0.09	0.40	0.34	0.15
10:λ_{max}	471	469	467	409	398	402	420
λ^{F}_{max}	554	563	574	582/485	490	–	423
Φ	0.17	0.15	0.08	0.10	0.10	0	0.04
11:λ_{max}	411	411	413	437	449	454	439
λ^{F}_{max}	463	467	464/524	530	530	531	476
Φ	0.03	0.03	0.03	0.04	0.04	0.05	0.04
12:λ_{max}	423	425	434	467	485	492	497/386
λ^{F}_{max}	493	493	494	590	603	608	–
Φ	0.16	0.17	0.10	0.03	0.01	0.01	0

The electronic properties of compounds **5**, **6** and **8**–**10** are dominated by the 2,5-bis(*p*-aminostyryl)pyrazine unit, substituents on the diphenylpyrazine axis only slightly modulating the acidochromic behavior. Protonation of DSP **5** starts in 10^{-3} M TFA, in 10^{-2} M TFA protonated **5** dominates the absorption spectrum (ca. 80%), and protonation is complete in 0.1 M TFA, 1 M TFA provoking a further protonation. In contrast to the previously discussed dyes, protonation causes a severe blueshift in the absorption maximum ($\Delta\lambda$ = 81 nm, $\Delta\tilde{\nu}$ = 3984 cm^{-1}), but this shift is reversed in highly concentrated TFA (λ_{max} = 411 nm, $\Delta\tilde{\nu}$ = 795 cm^{-1}). Acid-induced changes in the fluorescence spectra occur at the same concentrations. The long-wavelength emission at λ_{max} = 561 nm is first weakened and slightly redshifted (10^{-3} M TFA: λ_{max} = 576 nm, $\Delta\tilde{\nu}^{F}$ = 464 cm^{-1}) and in 10^{-2} M TFA is transformed into a more hypsochromic emission with λ_{max} = 443 nm ($\Delta\tilde{\nu}^{F}$ = 4784 cm^{-1}). A further increase in TFA concentration leads to a redshift of this intense emission (1 M TFA: λ_{max} = 482 nm, $\Delta\tilde{\nu}^{F}$ = 1826 cm^{-1}). The impact of TFA on the absorption spectra of **8**–**10** is very similar, only minor variations of shifts and basicities were found. Dye **6** with aza-crown end-groups is significantly more prone to protonation in its excited state than its congeners: Even in 10^{-5} M TFA, the spectrum is dominated by the emission of protonated **6** with residual emission of neutral **6**. This maximum disappears only at TFA $\geq 10^{-3}$ M and the redshift of the maximum (**6**: $\Delta\tilde{\nu}$ = 1679 cm^{-1}) is significantly larger than that observed for **5** and **8**–**10**.

The changes in the electronic spectra of **1**–**12** result from protonation of the amines or azines. These dyes can also act as ligands for metal ions. Two preliminary results may illustrate the effect of cations on the electronic spectra. Upon addition of Fe^{3+} (0.13–1.25 equiv.) to **3** in CH_2Cl_2, the band at λ = 418 nm vanishes gradually and a new band at λ = 549 nm appears; the emission is simultaneously quenched. The absorption spectra show an isosbestic point at λ = 461 nm. Crown ether **6** is capable of chelating Na^+ and Ca^{2+}: The absorption maxima are hypsochromically shifted from λ = 470 to 412 nm ($NaClO_4$, $\Delta\tilde{\nu}$ = –2995 cm^{-1}) and λ = 404 nm [$Ca(ClO_4)_2$, $\Delta\tilde{\nu}$ = –3496 cm^{-1}], and the emission shifts from λ = 536 to 530 nm ($NaClO_4$, $\Delta\tilde{\nu}^{F}$ =

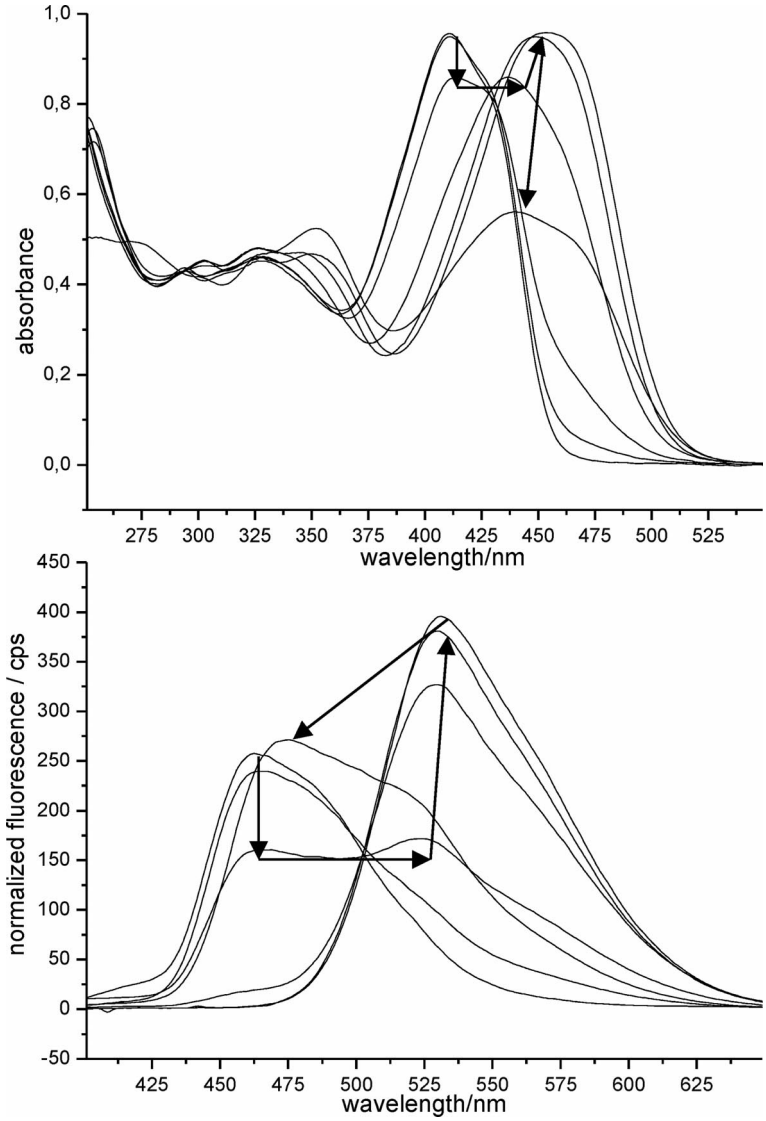

Figure 3. Electronic spectra of **11** in DCM with increasing concentrations of TFA (upper spectra: absorption; lower spectra: emission, normalized to identical optical density at λ^{exc} = 345 nm; cps = counts s^{-1}).

–211 cm^{-1}) and 523 nm [$Ca(ClO_4)_2$, $\Delta\tilde{\nu}^F$ = –464 cm^{-1}]. The metal-sensing properties of these fluorophores are currently under investigation.

Discussion

Solvatochromism

In accord with the formal C_2 symmetry of **1**–**12**, the solvatochromism of the absorption is only weak. Nevertheless, Table 4 reveals that the strong amine donors in DSPs **5**, **6** and **8**–**10** significantly enhance the solvatochromic response $\Delta\tilde{\nu}^{Abs}$ of the DSPs in the absorption spectra. Fluorescence gives a more refined picture: $\Delta\tilde{\nu}^F$ is small for DSPs with terminal acceptors (**1**, **2**, **11**, **12**: $\Delta\tilde{\nu}^F$ = 336–510 cm^{-1}), increases with moderate donors (**3**, **4**, **7**: $\Delta\tilde{\nu}^F$ = 1022–1668 cm^{-1}), and amino groups cause the largest shifts (**5**, **6**, **8**–**10**: $\Delta\tilde{\nu}^F$ = 2134–2411 cm^{-1}). This corresponds to a favorable charge transfer from the donors to the central pyrazine and a significant stabilization of the excited state. The influence of aryl groups on the pyrazine is less pronounced: Electron-donating anisyl strengthens the solvatochromism of a quinolyl-DSP (**11** vs. **12**) but weakens that of amino-DSPs (**5** vs. **9**).

Changes in the charge distribution and geometry on going from the ground to the excited state are reflected in the Stokes shifts ($\Delta\tilde{\nu}^{St}$) of the fluorophores. As the polarity increases, so the $\Delta\tilde{\nu}^{St}$ increases if the excited-state dipole moment is larger than that of the ground state.[23] DSPs **1**–**12** are formally centrosymmetric, but judged on the basis of geometric parameters, conjugation through one of the two arms is preferred. Although this may be due to packing, electro-optical absorption measurements on related distyrylpyrazines[24] in solution revealed that these molecules have a dipole moment that increases strongly upon excitation. These dipole moments result from the breaking of

Table 4. Solvatochromic shifts $\Delta\tilde{\nu}$ (cyclohexane – acetonitrile), correlation of $\Delta\tilde{\nu}^F$ (E^T_N) and $\Delta\tilde{\nu}^{St}$ (Δf), and changes in the dipole moments $\Delta\mu$ of **1**–**12**.

DSP	Solvatochromic shifts			$\tilde{\nu}^F$ (E^T_N)	Lippert–Mataga: $\Delta\tilde{\nu}^{St}$ (Δf)		
	$\Delta\tilde{\nu}^{Abs}$ [cm^{-1}]	$\Delta\tilde{\nu}^F$ [cm^{-1}]	$\Delta\Delta\tilde{\nu}$ [cm^{-1}]	m [cm^{-1}]	m [cm^{-1}]	y [cm^{-1}]	$\Delta\mu_{ge}$ [D]
1	–63	402	465	–891	1527	2493	7.6
2	–62	336	398	–805	1557	2593	12.8
3	58	1053	995	–2266	3067	2322	14.1
4	–116	1668	1784	–3555	5325	2843	26.2
5	965	2376	1411	–5269	4282	2120	16.2
6	610	2135	1525	–4268	4014	2084	15.7
7	–59	1022	1081	–2167	3275	2201	14.5
8	1125	2411	1286	–5293	5965	1466	19.2
9	925	2253	1328	–4950	4075	2123	15.8
10	665	2289	1624	–4863	4864	2322	17.3
11	–60	378	438	–649	1109	2653	9.6
12	0	510	510	–881	1481	4899	11.1

the formal centrosymmetry[25] in their ground states and from localized excitations in their Franck–Condon states.

The order of increasing solvatochromic sensitivity of the fluorescence of **1**–**12** can be obtained from a correlation of the emission maxima with a polarity parameter. "Solvent polarity" is a property that results from different influences of the individual solvent. Among the large number of polarity scales, Reichardts E^N_T is probably most established.[26] To estimate the relationship $\Delta\tilde{\nu}^F(E^N_T)$, ethanol was omitted because it is a hydrogen-bond donor (HBD). The solvatochromic shifts of the DSPs observed in protic solvents deviate significantly from those obtained in non-HBD solvents.[27] The results of a linear regression of the emission maxima $\tilde{\nu}^F$ and E^N_T are collected in Table 4: The slope m reflects the polarity-induced stabilization of the excited states of the chromophores. The fluorescence of the acceptor-substituted DSPs is less influenced by polarity than the fluorescence of DSPs with alkoxy donors, with amino-substituted dyes showing the highest sensitivity. The variation in m (**11** < **2** < **12** < **1** < **7** < **3** < **4** < **6** < **10** < **9** < **5** < **8**) also reflects the influence of substitution on the teraryl axis: Donors on acceptor-substituted DSPs enhance the sensitivity (**11** < **12**) but reduce it if the π system is donor-substituted (**10** < **9** < **5**).

A more detailed study of the different influences of solvent properties on the solvatochromic shifts of this class of dyes was performed on representative chromophores: The fundamental dye **1**, **4** with terminal carbazole donors, the cruciform **10** with amino and carbazolyl groups, and **11** with quinoline end-groups. The solvatochromism of the electronic spectra results from the interplay of different solvent characteristics with the initial and Franck–Condon states of the chromophore. Catalán[29] developed a multiparameter scale to analyze the contributions of solvent properties, which is given by Equation (1) in which A is the solvent-dependent property of a solute in a given solvent and results from the sum of this property of the solute in the gas phase A_0 and the contributions of the solvent effects caused by solvent acidity SA, solvent basicity SB, solvent dipolarity SdP, and solvent polarizability SP weighted by the regression coefficients b to e describing the sensitivity of property A to the different solute–solvent interactions.

$$A = A_0 + b\mathrm{SA} + c\mathrm{SB} + d\mathrm{SP} + e\mathrm{SdP} \quad (1)$$

By using this approach to elucidate the solvatochromism, we can conclude that the solvent polarizability SP is by far the most important contribution to the solvatochromism of the excitation ($|d| >> |b|, |c|, |e|$). The vibrational relaxation of the Franck–Condon state to the emitting state results in geometrical reorganization of the solute and the solvent shell.[30] Solvent dipoles are reorganized according to the charge distribution in the excited solute molecule thus stabilizing the emitting state. Accordingly, the multiparameter analysis of the emission reveals that in addition to the polarizability SP, the solvent acidity SA and the solvent dipolarity SdP significantly contribute to the solvatochromism. The impact of solvent acidity on the fluorescence increases with donor substitution on the distyryl segment (**11** < **1** < **4** < **10**). The same sequence is valid for the impact of solvent dipolarity SdP on the emission. Note that the impact of dipolarity exceeds the contribution of solvent polarizability only when the DSP is substituted with the very strong EPD dialkylamino group (**10**).

The Lippert–Mataga equation [Equation (2)][31] relates solvatochromic shifts $\Delta\tilde{\nu}^{St}$, the orientation polarizability Δf, and the cavity radius a, and allows calculation of the change in the dipole moment $\Delta\mu_{ge}$ on going from the ground to the excited states. To estimate $\Delta\mu_{ge}$, the diameter $2a$ of the cavity was approximated to the length of the π system,[22] thus reflecting the lower limit of the diameter of a spherical solvent cage. The results are collected in Table 4. Like the solvatochromic sensitivity of **1**–**12**, their dipole moments in the excited state μ_e increase with enhanced donor strength on the terminal positions. Alkoxy donors (**3**, **7**) are significantly less effective than amino donors (**4**–**6**, **8**–**10**). The largest value for $\Delta\mu_{ge}$ was obtained for **4**, in part due to the larger value of a = 10.9 Å. Recently we obtained the dipole moments μ_g = 4.4 D and μ_e = 47.0 D for **5** from electro-optical absorption measurements.[24] The different results obtained by the solvatochromic ($\Delta\mu_{ge}$ = 16.2 D) and EOAM methods ($\Delta\mu_{ge}$ = 42.6 D) can be accounted for by the following two reasons. First, EOAM compares ground and Franck–Condon states in the absorption process whereas the Lippert–Mataga method ($\Delta\mu_{ge}$ = 16.2 D) in-

cludes the relaxation from the Franck–Condon state to the emitting state and the emission process. Secondly, the Onsager radius of the cavity a is a crucial value:[32] To obtain the minimal values for $\Delta\mu_{ge}$ we approximated a spherical cavity with the radius a being half the length of the π system $2a$. If the Onsager radius of the more ellipsoidal cavity is approximated as $0.7 \times 2a$,[33] much larger values for $\Delta\mu_{ge}$ result, for example, $\Delta\mu_{ge}$ = 26.8 D for **5**. Furthermore, $2a$ was approximated as the length of the π system, the entire molecule is longer, thus resulting in even greater changes in the dipole moment. Besides the Onsager radius, two more aspects should be mentioned: 1) The evaluation of the solvatochromism by the Lippert–Mataga method is based on the orientation polarizability Δf, but solvent dipolarity also contributes to the solvatochromic shifts (compare eSdP in Table 5) and 2) although significant dipole moments of centrosymmetrical chromophores in their excited states have been reported,[34] their solvatochromic shift has not yet become a standard tool.[35] Nevertheless, even with these imponderabilities, these dyes exhibit large dipole moments in the excited states in spite of their formal centrosymmetry.

$$\Delta\tilde{\nu} = \tilde{\nu}_a - \tilde{\nu}_g = \frac{2\,(\mu_e - \mu_g)^2}{h \cdot c \cdot a^3} \cdot \Delta f + \text{const.} \qquad (2)$$

Table 5. Solvatochromic shifts of **1**, **4**, **10**, and **11**, and data from Cataláns multiparameter analysis.[28]

Solvent	**1** λ^{Abs} [nm]; λ^{F} [nm]	**4** λ^{Abs} [nm]; λ^{F} [nm]	**10** λ^{Abs} [nm]; λ^{F} [nm]	**11** λ^{Abs} [nm]; λ^{F} [nm]
n-Heptane	396; 441	414; 461	451; 501	408; 458
Methylcyclohexane	397; 443	412; 464	453; 505	408; 460
Cyclohexane	398; 442	416; 463	452; 505	408; 456
1,4-Dioxane	399; 445	417; 476	462; 528	410; 461
Triethylamine	398; 441	409; 466	456; 495	409; -
Toluene	402; 447	422; 475	467; 527	412; 463
Benzene	402; 439	422; 477	469; 509	413; 463
Dichloromethane	401; 452	419; 490	471; 554	411; 463
Ethyl acetate	398; 442	413; 476	463; 513	408; 460
Acetonitrile	397; 450	414; 502	466; 571	407; 464
Dimethylacetamide	402; 450	419; 501	476; 551	413; 465
Dimethyl sulfoxide	403; 452	420; 500	480; 562	414; 468
2-Propanol	398; 451	414; 488	463; 551	407; 462
Ethanol	398; 453	412; 493	464; 580	407; 463
Methanol	397; 456	411; 516	467; 570	406; 464
Abs $\tilde{\nu}_0$ [cm^{-1}]	26631	26049	24790	26005
Abs SA: b [cm^{-1}]	–144	–101	–417	–45
Abs SB: c [cm^{-1}]	–36	262	29	34
Abs SP: d [cm^{-1}]	–2189	–2894	–4143	–2252
Abs SdP: e [cm^{-1}]	–15	–92	–625	3
EM: $\tilde{\nu}^{F}_0$ [cm^{-1}]	23110	22853	20959	22684
EM SA: b [cm^{-1}]	–783	–1626	–1959	–250
EMSB: c [cm^{-1}]	116	398	665	66
EM SP: d [cm^{-1}]	–726	–2135	–1835	–1300
EM SdP: e [cm^{-1}]	–417	–1365	–2128	–256

Acidochromism

The weak basicity of the pyrazine unit in **1** increases upon charge transfer in the excited state.[36] The redshifted electronic transitions result from protonation on the heterocycle (pyrazine: pK_B = 13.4[37]), thus enhancing its acceptor strength. Accordingly, cyano-substitution (**2**) reduces the basicity and it was expected that EPD substituents would enhance the basicity. But the protonation of **3** and **4** requires higher TFA concentrations than **1**; the main effects of donor substitution are a largely enhanced redshift of the absorption band and a quenching of the fluorescence because these protonated DSPs are not emissive. An exchange of the central phenyl substitution (**3**) to α-naphthyl (**7**) results in similar redshifts but enhanced basicity: 10^{-2} M TFA is sufficient to protonate the majority of **7**. The pyrazine N in **3** acts as a ligand for Lewis acidic Fe^{3+}, and even with concentrations as low as 10^{-7} M, a new band at λ = 549 nm appears.

Because quinoline has a higher basicity (pK_B = 9.13),[37] protonation of DSPs **11** and **12** starts in 10^{-4} M TFA. Protonation of the quinoline is supported by NMR spectroscopy. The protons of the quinoline and 1-H of the vinylene bridge are strongly shifted ($\Delta\delta \leq 0.6$ ppm) to lower fields upon addition of TFA. The initial redshifts of the absorption bands of dipolar protonated **11** and **12** ($\Delta\lambda$ = 43 and 69 nm) are reversed upon transfer of a proton to the second quinoline unit in 1 M TFA. With methoxy as EPD substituents on the central phenyl rings (**12**), the electronic transitions are shifted to lower energies and, whereas protonated **11** is highly emissive, the fluorescence in **12** is quenched.

Similarly to these dyes, the terminal amino groups in **5**, **6**, and **8**–**10** are the preferred sites for protonation. Protonation results in large hypsochromic shifts of the absorption ($\Delta\lambda$ = 73–89 nm) followed by small redshifts in 1 M TFA ($\Delta\lambda$ = 29–90 nm). Protonation transforms strong EPD amines into weak electron-withdrawing ammonium ions. The large blueshifts indicate that both amino groups in **5**, **6**, and **8**–**10** are simultaneously protonated and the transition energies (λ_{max} = 393–414 nm) are similar to that of the fundamental dye **1** (λ_{max} = 401 nm in DCM). The redshifts in 1 M TFA result from further protonation of the pyrazine. Although the absorption spectra show the neutral and two protonated forms of **5**, **6**, and **8**–**10**, fluorescence shows four species: Small concentrations of TFA lead to a redshifted emission, best visible in the spectra of aza-crown substituted **6**. This accounts for a monoprotonated dye. The second protonation of the excited dyes or excitation of the twofold protonated dyes gives rise to a strongly blueshifted emission ($\Delta\lambda$ = 84–119 nm). Cations like Na^+ and Ca^{2+} are chelated by the aza-crown of **6** but the hypsochromic shifts are less pronounced because these ions interact with several donor atoms in the crown. The transition energies of diprotonated **5**, **6**, and **8**–**10** are similar to those of the neutral fundamental dye **1**. In 1 M TFA, the fourth emitting species of **5**, **6**, and **8**–**10** result from protonation of the pyrazine. With $\Delta\lambda^F$ = 29–90 nm, these bathochromic shifts adopt an intermediate position between those observed by protonation of cyano-substituted **2** ($\Delta\lambda^F$ = 34 nm) and **1**, which lacks a terminal acceptor ($\Delta\lambda^F$ = 127 nm).

Conclusions

A series of centrosymmetric diaryldistyrylpyrazines have been prepared, and the optical properties of these fluorophores have been studied. The influence of diaryl substitution the central pyrazine on absorption and fluorescence spectra is only small because the conjugation through the distyrylpyrazine is favored. A positive solvatochromism of the emission indicates a highly dipolar excited state. According to the solvatochromic method, excitation leads to an increase in the dipole moments of about 9–16 D. DSPs with or without non-basic donors on the styryl termini are protonated on the central pyrazine ring resulting in bathochromism of the absorption and emission and gradually quenched fluorescence. Two kinds of basic sites on the styryl axis were studied: Quinolyl end-groups are more basic than the pyrazine, protonation resulting in bathochromism of the absorption and emission, but with dialkylamino groups an initial strong hypsochromism of the two maxima is followed by bathochromism. These fluorophores are interesting for sensing applications because their absorption and emission properties are strongly affected by environmental conditions such as polarity, pH, and the presence of cations.

Experimental Section

General: All the reactions were carried out under dry nitrogen unless otherwise indicated. Commercially available reagents were used without further purification; solvents were dried by standard procedures, yields refer to chromatographically and spectroscopically pure compounds unless otherwise stated. ^{1}H and ^{13}C NMR spectra: Bruker AC 300 (300 MHz), AV 400 (400 MHz), and ARX 400 (400 MHz) spectrometers in $CDCl_3$ and [D_6]DMSO. ^{1}H and ^{13}C NMR signals were assigned on the basis of DEPT, COSY 45, HMQC, and HMBC experiments. Chemical shifts: δ values are in ppm, coupling constants are in Hz. Abbreviations: Pz = pyrazine, Ph = phenyl, Ph-p = phenyl attached to pyrazine, Cb = carbazole, vin = vinyl, Np = naphthyl, Qu = quinolyl, br. = broad signal, sup. = superimposed signals. Melting points: Tottoli apparatus (Büchi). IR spectra: Beckman Acculab 4 or JASCO 4100 FT-IR (ATR). MS (FD) spectra: Finnigan Mat 95 spectrometer. HR-ESI-MS: Q-TOF-ULTIMA 3 spectrometer with Lock Spray device (Waters-Micromass) and NaICsI Standard as reference. UV/Vis spectra: Perkin–Elmer Lambda 16 spectrophotometer; fluorescence spectra: Perkin–Elmer LS 50B spectrophotometer. Fluorescence spectra are normalized to identical optical density at the excitation wavelength of 350 nm. Fluorescence quantum yields (+/– 20%) were obtained by comparison with quinine sulfate in 0.1 M H_2SO_4 (Φ = 0.577).[38] Elemental analyses: Vario EL.

The starting materials were prepared according to literature methods: 1-(4-Bromophenyl)propan-2-one[39] (**13b**), 1-naphthylpropan-2-one[40] (**13d**), 1-hydroxyimino-1-phenylpropan-2-one[41] (**14a**), *p*-octyloxybenzaldehyde[42] (**18b**), 4-(9-carbazolyl)benzaldehyde[14e] (**18c**), 4-(*N*,*N*-dipropylamino)benzaldehyde[43] (**18d**), 4-(4′,7′,10′,13′-tetraoxa-1-azacyclopentadecyl)benzaldehyde[44] (**18e**), 4-hexyloxybenzaldehyde[45] (**18f**), diethyl 4-cyanobenzylphosphonate[46] (**20a**) and diethyl quinolylmethylphosphonate[47] (**20b**).

(*E*,*E*)-2,5-Distyryl-3,6-diphenylpyrazine (1): KO*t*Bu (205 mg, 1.84 mmol) was added to a stirred solution of **17a** (160 mg, 0.61 mmol) and benzaldehyde (196 mg, 1.84 mmol) in DMF (30 mL) under N_2. After 30 min at 0 °C and 4 h at 25 °C, water (80 mL) was added and **1** was extracted with $CHCl_3$ (3 × 50 mL). The combined organic solutions were washed with brine, dried ($MgSO_4$), concentrated, and purified by chromatography to give 170 mg (0.39 mmol, 64%) of a yellow solid with m.p. 268–269 °C. ^{1}H NMR ($CDCl_3$, 300 MHz, 25 °C): δ = 7.97 (d, ^3J = 15.7 Hz, 2 H, 2-H vin), 7.85 (d, ^3J = 6.9 Hz, 4 H, 2-H, 6-H Ph-vin), 7.6–7.5 (m, 10 H, 3-H, 4-H, 5-H Ph-vin, 2-H, 6-H Ph-p), 7.38–7.26 (m, 8 H, 3-H vin, 3-H, 4-H, 5-H Ph-p) ppm. ^{13}C NMR ($CDCl_3$, 75 MHz, 25 °C): δ = 150.1 (C-2 Pz), 145.0 (C-1 Pz), 138.0 (C-1 Ph-p), 136.8 (C-1 Ph-vin), 134.8 (C-2 vin), 130.0 (C-2, C-6 Ph-p), 129.0 (C-4 Ph-vin), 128.7 (C-3, C-5 Ph-vin), 128.5 (C-3, C-5 Ph-p), 128.4 (C-4 Ph-p), 127.3 (C-2, C-6 Ph-vin), 124.0 (C-1 vin) ppm. IR (ATR): $\tilde{\nu}$ = 3056, 1625, 1495, 1449, 1382, 1203, 1134, 1024, 963, 765, 752 cm^{-1}. MS (FD): *m*/*z* (%) = 436.6 (100) [M]$^+$. HRMS: calcd. for $C_{32}H_{25}N_2^+$ 437.2018 [M + H]$^+$; found 437.2023.

(*E*,*E*)-2,5-Bis[2-(4-cyanophenyl)ethenyl]-3,6-diphenylpyrazine (2): Phosphonate **20a** (148 mg, 0.58 mmol) and **18a** (70 mg, 0.24 mmol) were dissolved in THF (30 mL) in a flame-dried flask. While stirring at 0 °C, KO*t*Bu (100 mg, 0.89 mmol) was added and after 30 min at 0 °C and 4 h at 25 °C, water (70 mL) was added, **2** was extracted with ethyl acetate (4 × 40 mL), and the combined organic solutions were washed with brine (2 × 30 mL), dried (Na_2SO_4), and concentrated. The residue was recrystallized from methanol/CH_2Cl_2 to yield 85 mg (0.17 mmol, 71%) of a yellow solid with m.p. 305 °C (dec.). ^{1}H NMR ($CDCl_3$, 400 MHz, 25 °C): δ = 7.97 (d, ^3J = 15.7 Hz, 2 H, 2-H vin), 7.80 (m, 4 H, 2-H, 6-H Ph-p), 7.64–7.56 (m, 14 H, 2-H, 3-H, 5-H, 6-H Ph-p), 7.43 (d, ^3J = 15.7 Hz, 2 H, 1-H vin) ppm. ^{13}C NMR ($CDCl_3$, 100 MHz): δ = 150.8 (C-3, C-6 Pz), 144.7 (C-2, C-5 Pz), 141.0 (C-1 Ph), 137.5 (C-1 Ph-p), 133.3 (C-2 vin), 132.5 (C-2, C-6 Ph), 129.9 (C-2, C-6 Ph-p), 129.5 (C-4 Ph-p), 128.7 (C-3, C-5 Ph-p), 127.7 (C-3, C-5 Ph), 127.3 (C-1 vin), 118.8 (CN), 111.5 (C-4 Ph) ppm. IR (KBr): $\tilde{\nu}$ = 3058, 2225, 1624, 1601, 1504, 1412, 1381, 1323, 1202, 1140, 1026, 970, 823, 701, 553 cm^{-1}. MS (FD): *m*/*z* (%) = 486.3 (100) [M]$^+$. HRMS: calcd. for $C_{34}H_{23}N_4$ 487.1923 [M + H]$^+$; found 487.1934.

(*E*,*E*)-2,5-Bis[2-(4-octyloxyphenyl)ethenyl]-3,6-diphenylpyrazine (3): According to the procedure for **1**, a solution of **17a** (150 mg, 0.50 mmol), **18b** (272 mg, 1.16 mmol), and KO*t*Bu (250 mg, 2.23 mmol) in DMF (20 mL) gave 250 mg (0.39 mmol, 67%) of a yellow solid with m.p. 170 °C. ^{1}H NMR ($CDCl_3$, 400 MHz, 25 °C): δ = 7.90 (d, ^3J = 15.6 Hz, 2 H, 2-H vin), 7.85–7.83 (m, 4 H, 2-H, 6-H Ph-p), 7.59–7.50 (m, 6 H, 3-H, 4-H, 5-H Ph-p), 7.42 (d, ^3J = 8.7 Hz, 4 H, 2-H, 6-H, Ph), 7.21 (d, ^3J = 15.6 Hz, 2 H, 1-H vin), 6.85 (d, ^3J = 8.7 Hz, 4 H, 3-H, 5-H Ph), 3.96 (t, 4 H, OCH_2), 1.78 (m, 4 H, β-CH_2), 1.45 (m, 4 H, γ-CH_2), 1.30 (m, 16 H, CH_2), 0.89 (t, 6 H, CH_3) ppm. ^{13}C NMR ($CDCl_3$, 75 MHz): δ = 159.5 (C-4 Ph), 149.8 (C-1 Pz), 145.0 (C-2 Pz), 138.4 (C-1 Ph-p), 134.2 (C-2 vin), 130.0 (C-2, C-6 Ph-p), 129.5 (C-3, C-5 Ph-p), 128.8 (C-4 Ph-p), 128.7, 128.4 (C-1, C-2, C-6 Ph), 121.8 (C-1 vin), 114.7 (C-3, C-5 Ph), 68.0 (OCH_2), 31.8 (β-CH_2), 29.4 (CH_2), 29.3 (2 CH_2), 26.0 (CH_2), 22.6 (CH_2), 14.1 (CH_3) ppm. IR (KBr): $\tilde{\nu}$ = 3060, 2923, 2853, 1625, 1604, 1385, 1285, 1246, 1173, 1135, 966, 819, 702 cm^{-1}. MS (FD): *m*/*z* (%) = 347.0 (1.8) [M]$^{2+}$, 692.2 (100) [M]$^+$. $C_{48}H_{56}N_2O_2$ (696.47): calcd. C 81.19, H 8.15, N 4.04; found C 80.86, H 7.99, N 3.92.

(*E*,*E*)-2,5-Bis{2-[4-(9-carbazolyl)phenyl]ethenyl}-3,6-diphenylpyrazine (4): According to the procedure for **1**, a solution of **17a** (100 mg, 0.38 mmol), **18c** (230 mg, 0.85 mmol), and KOH (100 mg, 1.78 mmol) in DMF (30 mL) gave 90 mg (0.12 mmol, 32%) of a bright-yellow solid that decomposed above 360 °C. ^{1}H NMR

($CDCl_3$, 400 MHz, 25 °C): δ = 8.15 (d, ^3J = 7.7 Hz, 4 H), 8.10 (d, ^3J = 15.7 Hz, 2 H), 7.91 (m, 4 H, 3-H), 7.74 (d, ^3J = 7.74 Hz, 4 H), 7.63 (m, 4 H), 7.60–7.56 (m, 6 H), 7.49–7.45 (m, 6 H), 7.42 (dt, ^3J = 8.2, ^4J = 1.2 Hz, 4 H), 7.30 (dt, ^3J = 7.7, ^4J = 1.3 Hz, 4 H) ppm. ^{13}C NMR ($CDCl_3$, 75 MHz, 25 °C): δ = 150.4, 145.0, 140.6, 138.0, 137.7, 135.9, 133.9, 130.0, 129.2, 128.7, 128.6, 127.1, 126.0, 124.8, 123.5, 120.3, 120.1, 109.8 ppm. IR (KBr): $\tilde{\nu}$ = 3055, 1624, 1600, 1514, 1478, 1451, 1361, 1316, 1228, 1169, 1138, 825, 748, 724, 700, 623 cm^{-1}. MS (FD): *m/z* (%) = 383.2 (6) $[M]^{2+}$, 766.2 (100) $[M]^+$. $C_{56}H_{38}N_4$ (766.93): calcd. C 87.79, H 4.99, N 7.31; found C 87.46, H 4.71, N 7.04.

(*E*,*E*)-2,5-Bis{2-[4-(dipropylamino)phenyl]ethenyl}-3,6-diphenylpyrazine (5): According to the procedure for **1**, a solution of **17a** (150 mg, 0.58 mmol), **18d** (260 mg, 1.27 mmol), and KO*t*Bu (250 mg, 2.23 mmol) in DMF (25 mL) gave 210 mg (0.33 mmol, 57%) of bright-orange crystals with m.p. 184–185 °C. ^{1}H NMR ($CDCl_3$, 400 MHz, 25 °C): δ = 7.86 (d, ^3J = 15.5 Hz, 2 H, 2-H, 2-H vin), 7.88–7.86 (m, 4 H, 2-H, 6-H Ph-p), 7.58–7.49 (m, 6 H, 3-H, 4-H, 5-H Ph-p), 7.37 (d, ^3J = 8.9 Hz, 4 H, 2-H, 6-H Ph), 7.14 (d, ^3J = 15.5 Hz, 2 H, 1-H vin), 6.60 (d, ^3J = 8.9 Hz, 4 H, 3-H, 5-H Ph), 3.27 (t, 8 H, NCH_2), 1.63 (m, 8 H, CH_2), 0.94 (t, 12 H, CH_3) ppm. ^{13}C NMR ($CDCl_3$, 75 MHz, 25 °C): δ = 149.3 (C-4 Ph), 148.3 (C-3, C-6 Pz), 144.9 (C-2, C-5 Pz), 138.8 (C-1 Ph-p), 134.3 (C-2 vin), 129.9 (C-2, C-6 Ph-p), 128.7 (C-3, C-5 Ph-p), 128.5 (C-2,C-6 Ph), 128.3 (C-4 Ph-p), 124.6 (C-1 Ph), 119.1 (C-1 vin), 111.4 (C-3, C-5 Ph), 52.8 (NCH_2), 20.5 (CH_2), 11.4 (CH_3) ppm. IR (KBr): $\tilde{\nu}$ = 2960, 2931, 2872, 1598, 1519, 1380, 1365, 1238, 1183, 1136, 809, 700 cm^{-1}. MS (FD): *m/z* (%) = 633.9 (100) $[M]^+$. HRMS (ESI): calcd. for $C_{44}H_{51}N_4$ 635.4114; found 635.4095.

X-ray Structure Determination of 5: Performed with an Enraf–Nonius Turbo-Cad 4 diffractometer equipped with a rotating anode using a red block. Crystal data: $C_{44}H_{50}N_4$, *M* 635 g mol^{-1}, 0.1 × 0.36 × 0.56 mm^3, triclinic, space group: $P\bar{1}$, Mo-K_α, graphite-monochromated 1.54180 Å, *T* = 193 K, unit cell dimensions: *a* = 9.2287(10), *b* = 13.058(14), *c* = 16.610(2) Å, α = 100.300(2), β = 105.007(2), γ = 102.174(2)°, *V* = 1831.3(6) $Å^3$, *z* = 2, $d_{calcd.}$ = 1.151 g cm^{-3}, absorption μ = 0.07 mm^{-1}, the θ range for data collection was 2–26°, index ranges: $-11 \le h \le 10$, $-16 \le k \le 15$, $-20 \le l \le 19$. Number of reflections collected: 13155; independent reflections: 6871 (R_{int} = 0.0216). The structure was solved by direct methods (program SIR92, refinement by SHELXL97).[48] Structure refinement was performed by full-matrix least-squares methods on 437 parameters, weighted refinement: $w = 1/[\sigma^2(F_o^2) + (0.0631P)^2 + 0.32P]$ with $P = [\max(F_o^2,0) + 2F_o^2]/3$ and hydrogen atoms located from difference Fourier synthesis and refined isotropically assuming a riding motion model, non-hydrogen atoms improved by anisotropic refinement. Goodness-of-fit on *S* = 1.026, maximal range of parameters 0.001 × e.s.d, final *R* indices: R_1 = 0.0490, wR_2 = 0.1378, the final difference Fourier map showed minimum and maximum values of 1.09 and –0.81 e $Å^{-3}$, respectively.

CCDC-918792 (for **5**) contains the supplementary crystallographic data for this paper. These data can be obtained free of charge from The Cambridge Crystallographic Data Centre via www.ccdc.cam.ac.uk/datarequest/cif.

(*E*,*E*)-2,5-Bis{2-[4-(4′,7′,10′,13′-tetraoxa-1-azacyclopentadecyl)-phenyl]ethenyl}-3,6-diphenylpyrazine (6): According to the procedure for **1**, a solution of **17a** (150 mg, 0.58 mmol), **18e** (175 mg, 1.56 mmol), and KO*t*Bu (100 mg, 1.78 mmol) in DMF (30 mL) gave 95 mg (0.11 mmol, 19%) of a red solid with m.p. 229–230 °C. ^{1}H NMR ($CDCl_3$, 400 MHz, 25 °C): δ = 7.86–7.82 (m, 6 H, 2-H vin, 2-H, 6-H Ph-p), 7.56–7.47 (m, 6 H, 3-H, 4-H, 5-H Ph-p), 7.36 (d, ^3J = 8.4 Hz, 4 H, 2-H, 6-H Ph), 7.12 (d, ^3J = 15.6 Hz, 2 H, 1-H vin), 6.61 (d, ^3J = 8.4 Hz, 4 H, 3-H, 5-H Ph), 3.76–3.60 (m, 40 H, CH_2) ppm. ^{13}C NMR ($CDCl_3$, 75 MHz): δ = 149.4, 147.7, 145.0 (C-4 Ph, C-3, C-6, C-2, C-5 Pz), 138.7 (C-1 Ph-p), 134.2 (C-2 vin), 129.9 (C-2, C-6 Ph-p), 128.8, 128.6, 128.3 (C-2, C-6 Ph, C-3, C-4, C-5 Ph-p), 124.9 (C-1 Ph), 119.5 (C-1 vin), 111.4 (C-3, C-5 Ph), 71.3, 70.2, 70.1 (OCH_2), 68.4 (N-CH_2CH_2), 52.6 (NCH_2) ppm. IR (ATR): $\tilde{\nu}$ = 2853, 1595, 1517, 1381, 1349, 1182, 1116, 958, 807, 762, 699 cm^{-1}. MS (FD): *m/z* (%) = 870.3 (100) $[M]^+$. $C_{52}H_{62}N_4O_8$ (871.08): calcd. C 71.70, H 7.17, N 6.43; found C 71.66, H 7.07, N 6.34.

(*E*,*E*)-2,5-Bis[2-(4-hexyloxyphenyl)ethenyl]-3,6-di(1-naphthyl)-pyrazine (7): According to the procedure for **1**, a solution of **17d** (150 mg, 0.42 mmol), **18f** (190 mg, 0.92 mmol), and KO*t*Bu (190 mg, 1.69 mmol) in DMF (30 mL) gave 85 mg (0.12 mmol, 29%) of bright-yellow needles with m.p. 156–158 °C. ^{1}H NMR ($CDCl_3$, 400 MHz, 25 °C): δ = 8.04 (d, ^3J = 8.2 Hz, 2 H, 4-H Np), 7.99 (d, ^3J = 8.0, ^4J = 1 Hz, 2 H, 5-H Np), 7.86 (br. d, ^3J = 8.0 Hz, 2 H, 8-H Np), 7.75 (d, ^3J = 15.7 Hz, 2 H, 2-H vin), 7.71 (br. d, ^3J = 7.4 Hz, 2 H, 2-H Np), 7.67 (t, ^3J = 7.4 Hz, 2 H, 3-H Np), 7.55 (dt, ^3J = 8.0, ^4J = 1.2 Hz, 2 H, 6-H Np), 7.50 (br. t, ^3J = 7.0 Hz, 2 H, 7-H Np), 7.13 (d, ^3J = 8.8 Hz, 4 H, 2-H, 6-H Ph), 6.76 (d, ^3J = 15.7 Hz, 2 H, 1-H vin), 6.69 (d, ^3J = 8.8 Hz, 4 H, 3-H, 5-H Ph), 3.98 (t, 4 H, OCH_2), 1.70 (m, 4 H, β-CH_2), 1.38 (m, 4 H, CH_2), 1.27 (m, 8 H, CH_2), 0.86 (t, 6 H, CH_3) ppm. ^{13}C NMR ($CDCl_3$, 75 MHz, 25 °C): δ = 159.4 (C-4 Ph), 150.4 (C-3, C-6 Pz), 147.0 (C-2, C-5 Pz), 135.9 (C-1 Np), 134.4 (C-2 vin), 133.9 (C-4a Np), 132.0 (C-8a Np), 129.3 (C-4 Np), 129.2 (C-1 Ph), 128.6 (C-2, C-6 Ph), 128.4 (C-2 Np), 128.3 (C-5 Np), 126.7 (C-7 Np), 126.2 (C-8 Np), 126.0 (C-6 Np), 125.4 (C-3 Np), 121.5 (C-1 vin), 114.5 (C-3, C-5 Ph), 67.9 (OCH_2), 31.5 (β-CH_2), 29.1, 25.6, 22.6 (CH_2), 14.0 (CH_3) ppm. IR (ATR): $\tilde{\nu}$ = 2923, 2852, 1603, 1572, 1245, 1174, 1025, 970, 823, 799, 771, 667 cm^{-1}. MS (FD): *m/z* (%) = 737.1 (100) $[M]^+$. $C_{52}H_{52}N_2O_2$ (736.98l): calcd. C 84.75, H 7.11, N 3.80; found C 84.40, H 7.69, N 3.51.

(*E*,*E*)-2,5-Bis{2-[4-(dipropylamino)phenyl]ethenyl}-3,6-di(1-naphthyl)pyrazine (8): According to the procedure for **1**, a solution of **17d** (150 mg, 0.42 mmol), **18d** (190 mg, 0.92 mmol), and KO*t*Bu (186 mg, 1.66 mmol) in DMF (40 mL) gave 65 mg (0.088 mmol, 21%) of an amorphous orange solid with m.p. 202–203 °C. ^{1}H NMR ($CDCl_3$, 400 MHz, 25 °C): δ = 8.03 (d, ^3J = 8.2 Hz, 2 H, 4-H Np), 8.00 (dd, ^3J = 8.1, ^4J = 1.1 Hz, 2 H, 5-H Np), 7.92 (br. d, ^3J = 8.0 Hz, 2 H, 8-H Np), 7.74 (br. d, ^3J = 6.7 Hz, 2 H, 1-H vin), 7.70 (d, ^3J = 15.6 Hz, 2 H, 2-H vin), 7.67 (t, 2 H, 3-H Np), 7.56 (dt, ^3J = 8.6, ^4J = 1.2 Hz, 2 H, 6-H Np), 7.50 (br. t, 2 H, 7-H Np), 7.07 (d, ^3J = 8.9 Hz, 4 H, 2-H, 6-H Ph), 6.66 (d, ^3J = 15.6 Hz, 2 H, 1-H vin), 6.43 (d, ^3J = 8.9 Hz, 4 H, 3-H, 5-H Ph), 3.17 (t, 8 H, NCH_2), 1.54 (m, 8 H, CH_2), 0.87 (t, 12 H, CH_3) ppm. ^{13}C NMR ($CDCl_3$, 100 MHz, 25 °C): δ = 150.0 (C-3, C-6 Pz), 148.2 (C-4 Ph), 146.9 (C-2, C-5 Pz), 136.4 (C-1 Np), 134.4 (C-2 vin), 133.8 (C-4a Np), 132.0 (C-8a Np), 128.9 (C-4 Np), 128.7 (C-2, C-6 Ph), 128.3 (C-2 Np), 128.2 (C-5 Np), 126.5 (C-7 Np), 126.2 (C-8 Np), 126.0 (C-6 Np), 125.4 (C-3 Np), 124.0 (C-1Ph), 118.9 (C-1 vin), 111.2 (C-3, C-5 Ph), 52.7 (NCH_2), 20.4 (CH_2), 11.3 (CH_3) ppm. IR (ATR): $\tilde{\nu}$ = 2922, 2852, 1596, 1518, 1390, 1363, 1178, 1135, 968, 801, 776 cm^{-1}. MS (FD): *m/z* (%) = 735.2 (100) $[M]^+$. HRMS: calcd. for $C_{52}H_{54}N_4$ 734.4348 $[M]^+$; found 734.4332.

(*E*,*E*)-2,5-Bis{2-[4-(dipropylamino)phenyl]ethenyl}-3,6-bis(4-methoxyphenyl)pyrazine (9): According to the procedure for **1**, a solution of **17c** (100 mg, 0.31 mmol), **18d** (155 mg, 0.76 mmol), and KO*t*Bu (170 mg, 1.52 mmol) in DMF (30 mL) gave 80 mg (0.12 mmol, 39%) of a red solid with m.p. 205–208 °C. ^{1}H NMR ($CDCl_3$, 400 MHz, 25 °C): δ = 7.82 (d, ^3J = 15.6 Hz, 2 H, 2-H vin), 7.79 (d,

^3J = 8.8 Hz, 4 H, 2-H, 6-H Ph-p), 7.36 (d, ^3J = 8.9 Hz, 4 H, 2-H, 6-H Ph), 7.11 (d, ^3J = 15.6 Hz, 2 H, 1-H vin), 7.06 (d, ^3J = 8.8 Hz, 4 H, 3-H, 5-H Ph-p), 6.58 (d, ^3J = 8.9 Hz, 4 H, 3-H, 5-H Ph), 3.92 (s, 6 H, OCH_3), 3.26 (t, 8 H, NCH_2), 1.61 (m, 8 H, CH_2), 0.93 (t, 6 H, CH_3) ppm. ^{13}C NMR ($CDCl_3$, 75 MHz, 25 °C): δ = 160.0 (C-4 Ph-p), 148.6, 148.2 (C-2, C-3, C-5, C-6 Pz), 144.6 (C-1 Ph-p), 133.9 (C-2 vin), 131.3 (C-2, C-6 Ph-p), 128.7 (C-2, C-6 Ph), 124.4 (C-1 Ph), 119.5 (C-1 vin), 113.8 (C-3, C-5 Ph-p), 111.4 (C-3, C-5 Ph), 1 C sup., 55.4 (OCH_3), 52.8 (NCH_2), 20.5 (CH_2), 11.4 (CH_3). IR (KBr): $\tilde{\nu}$ = 2960, 2931, 2873, 1600, 1519, 1379, 1364, 1295, 1249, 1183, 1137, 1032, 837, 810 cm^{-1}. MS (FD): *m*/*z* (%) = 347.5 (1) $[M]^{2+}$, 694.1 (100) $[M]^+$. HRMS: calcd. for $C_{46}H_{54}N_4O_2$ 694.4247 $[M]^+$; found 694.4225.

(*E*,*E*)-2,5-Bis[4-(9-carbazolyl)phenyl]-3,6-bis{2-[4-(dimethylamino)-phenyl]ethenyl}pyrazine (10): 4-Dimethylaminobenzaldehyde (1.00 g, 6.7 mmol) and KO*t*Bu (750 mg, 6.7 mmol) were dissolved in DMF (30 mL) under N_2 and **17e** (120 mg, 0.2 mmol) was added slowly to the stirred mixture. Stirring was continued for 4 h, water (100 mL) was added, and the product extracted with $CHCl_3$ (4 × 50 mL). The combined organic solutions were washed with brine (3 × 30 mL), dried ($MgSO_4$), concentrated, and recrystallized from CH_2Cl_2/methanol, yield 135 mg (0.16 mmol, 78%) of orange crystals with m.p. 347 °C. ^1H NMR ($CDCl_3$, 400 MHz, 25 °C): δ = 8.20 (d, ^3J = 7.8 Hz, 4 H, 4-H, 5-H Cb), 8.16 (d, ^3J = 8.4 Hz, 4 H, 2-H, 6-H Ph-p), 8.01 (d, ^3J = 15.5 Hz, 2 H, 2-H vin), 7.80 (d, ^3J = 8.4 Hz, 4 H, 3-H, 5-H Ph-p), 7.63 (d, ^3J = 8.2 Hz, 4 H, 1-H, 8-H Cb), 7.52–7.48 (m, 8 H, 2-H, 6-H Ph, 2-H, 7-H Cb), 7.36 (t, 4 H, 3-H, 6-H Cb), 7.32 (d, ^3J = 15.5 Hz, 2 H, 1-H vin), 6.72 (d, ^3J = 8.9 Hz, 4 H, 3-H, 5-H Ph), 3.00 (s, 12 H, NCH_3) ppm. ^{13}C NMR ($CDCl_3$, 75 MHz): δ = 150.7 (C-2, C-5 Pz), 148.6 (C-4 Ph), 145.1 (C-3, C-6 Pz), 140.7 (C-1 Ph-p), 138.2 (C-4a, C-4b Cb), 137.6 (C-4 Ph-p), 135.2 (C-2 vin), 131.5 (C-3, C-5 Ph-p), 128.8 (C-2, C-6 Ph), 126.8 (C-2, C-6 Ph-p), 126.1 (C-2, C-7 Cb), 125.1 (C-1 Ph), 123.6 (C-8a, C-9a Cb), 120.4 (C-4, C-5 Cb), 120.1 (C-3, C-6 Cb), 119.2 (C-1 vin), 112.2 (C-3, C-5 Ph), 110.0 (C-4 Ph), 40.3 (CH_3) ppm. IR (ATR): $\tilde{\nu}$ = 2920, 2851, 1601, 1517, 1449, 1354, 1222, 1186, 1165, 1073, 807, 742, 721 cm^{-1}. MS (FD): *m*/*z* (%) = 426.2 (7) $[M]^{2+}$, 852.0 (100) $[M]^+$, 1572.5 (1.2) $[M_2]^+$. $C_{60}H_{48}N_6$ (853.08): calcd. C 84.48, H 5.67, N 9.85; found C 84.14, H 5.83, N 9.59.

(*E*,*E*)-2,5-Bis[2-(2-quinolyl)ethenyl]-3,6-diphenylpyrazine (11): According to the procedure for **1**, a solution of **19a** (200 mg, 0.69 mmol), **20b** (419 mg, 1.5 mmol) in abs. THF (50 mL), and KO*t*Bu (233 mg, 2.08 mmol) yielded 180 mg (48%) of orange needles with m.p. 301 °C. ^1H NMR ($CDCl_3$, 400 MHz): δ = 8.27 (d, ^3J = 15.6 Hz, 2 H, 1-H vin), 8.09 (d, ^3J = 8.6 Hz, 2 H, 4-H Qu), 8.07 (d, ^3J = 8.6 Hz, 2 H, 8-H Qu), 7.95 (d, ^3J = 15.6 Hz, 2 H, 2-H vin), 7.90 (m, 4 H, 2-H, 6-H Ph), 7.77 (dd, ^3J = 8.1, ^4J = 1.4 Hz, 2 H, 5-H Qu); 7.68 (dt, ^3J = 8.6, ^4J = 1.4 Hz, 2 H, 7-H Qu), 7.64–7.55 (m, 8 H, 3-H Qu, 3-H, 4-H, 5-H Ph), 7.49 (dt, ^3J = 8.1, ^4J = 1.1 Hz, 2 H, 6-H Qu) ppm. ^{13}C NMR ($CDCl_3$, 75 MHz): δ = 155.5 (C-2 Qu), 150.8 (C-2, C-5 Pz), 148.4 (C-8a Qu), 144.9 (C-3, C-6 Pz), 137.7 (C-1 Ph), 136.3 (C-4 Qu), 135.5 (C-2 vin), 130.2 (C-2, C-6 Ph), 129.8, 129.7, 129.5, 129.2 (C-1 vin, C-7, C-8 Qu, C-4 Ph), 128.5 (C-3, C-5 Ph), 127.6, 127.5, 126.5 (C-4a, C-5, C-6 Qu), 120.0 (C-3 Qu) ppm. IR (KBr): $\tilde{\nu}$ = 3057, 1628, 1594, 1505, 1426, 1384, 1205, 1134, 974, 822, 754, 699, 620 cm^{-1}. MS (FD): *m*/*z* (%) = 598.4 (100) $[M]^+$. HRMS (ESI): calcd. for $C_{38}H_{27}N_4$ 539.2236; found 539.2230.

(*E*,*E*)-2,5-Bis[2-(2-quinolyl)ethenyl]-3,6-bis(4-methoxyphenyl)-pyrazine (12): Similar to the preparation of **11**, **19c** (30 mg, 0.086 mmol), and **20b** (60 mg, 0.21 mmol) gave 44 mg (85%) of a poorly soluble yellow solid that decomposed at 330 °C. ^1H NMR ($CDCl_3$, 400 MHz): δ = 8.25 (d, ^3J = 15.6 Hz, 2 H, 1-H vin), 8.12 (d, ^3J = 8.6 Hz, 2 H, 4-H Qu), 8.08 (d, ^3J = 8.6 Hz, 2 H, 8-H Qu), 7.96 (d, ^3J = 15.6 Hz, 2 H, 2-H vin), 7.88 (d, ^3J = 8.8 Hz, 4 H, 2-H, 6-H Ph), 7.78 (d, ^3J = 8.1 Hz, 2 H, 5-H Qu), 7.71 (dt, ^3J = 8.6, ^4J = 1.4 Hz, 2 H, 7-H Qu), 7.65 (d, ^3J = 8.6 Hz, 2 H, 3-H Qu), 7.51 (dt, ^3J = 8.1, ^4J = 1.1 Hz, 2 H, 6-H Qu), 7.12 (d, ^3J = 8.8 Hz, 4 H, 3-H, 5-H Ph), 3.95 (s, 6 H, OCH_3) ppm. IR (KBr): $\tilde{\nu}$ = 3057, 2929, 2836, 1654, 1608, 1595, 1517, 1505, 1426, 1409, 1384, 1303, 1251, 1204, 1175, 1136, 1030, 980, 838, 823, 756, 620 cm^{-1}. MS (FD): *m*/*z* (%) = 598.4 (100) $[M]^+$. HRMS (ESI): calcd. for 599.2447 $C_{40}H_{31}N_4O_2$; found 599.2473.

1-Hydroxyimino-1-(4-bromophenyl)propan-2-one (14b): Similar to the procedure for **14c** (see below), ethyl acetoacetate (20 g, 0.15 mol), 4-bromoaniline (25.0 g, 0.15 mol), $NaNO_2$ (2 × 10.0 g, 2 × 0.15 mol), and KOH (8.6 g, 0.15 mol) gave 20.5 g (84.7 mmol, 55%) of light-brown crystals with m.p. 190 °C. The same product was obtained from **13b** (6.5 g, 30.5 mmol) in diethyl ether (50 mL), HCl (1 mL), and isoamyl nitrite (4.5 g, 38 mmol) following the procedure given for **14d** (see below), yield 4.0 g (16.5 mmol, 54%). ^1H NMR ($CDCl_3$, 300 MHz, 25 °C): δ = 11.97 (s, 1 H, OH), 7.33 (d, ^3J = 8.6 Hz, 2 H, 3-H, 5-H), 7.02 (d, ^3J = 8.6 Hz, 2 H, 2-H, 6-H), 2.32 (s, 3 H, CH_3) ppm. ^{13}C NMR ($CDCl_3$, 75 MHz, 25 °C): δ = 196.5 (C=O), 154.5 (C=N), 131.0, 130.6 (C-2, C-3, C-5, C-6), 127.9 (C-1), 122.8 (C-Br), 25.8 (CH_3) ppm. IR (KBr): $\tilde{\nu}$ = 3032, 2924, 2860, 1661, 1591, 1490, 1435, 1396, 1367, 1309, 1298, 1187, 1073, 995, 935, 819, 631 cm^{-1}. MS (FD): *m*/*z* (%) = 240.9 (100) $[M]^+$.

1-Hydroxyimino-1-(4-methoxyphenyl)propan-2-one (14c): A solution of 4-methoxyphenyldiazonium sulfate was prepared from $NaNO_2$ (5.1 g, 73.9 mmol) in water (20 mL) and *p*-anisidine (9.0 g, 73.1 mmol) in H_2SO_4 (20%, 40 mL). A second solution was prepared from ethyl acetoacetate (9.5 g, 0.073 mol) and KOH (4.1 g, 0.077 mol) in water (45 mL). This was stirred for 3 h before $NaNO_2$ (5.1 g, 0.074 mol) was added. The mixture was then cooled to 0 °C and H_2SO_4 (30%, 25 mL) was added dropwise. After vigorous stirring for 30 min, $CuSO_4 \cdot 5H_2O$ (1.9 g, 7.7 mmol) in water (20 mL) and $Na_2S_2O_5$ (4.4 g, 0.023 mol) in water (10 mL) were added followed by the solution of the diazonium salt. Vigorous stirring was continued for 3 h at ambient temperature. The mixture was saturated with NaCl and the precipitate collected by filtration through a Büchner funnel. The residue was dissolved in NaOH (2.5 M), filtered, and precipitated by addition of glacial acetic acid. Suction filtration, dissolution in dichloromethane, drying ($MgSO_4$), evaporation, and recrystallization from toluene gave 3.8 g (19.7 mmol, 27%) of an off-white solid with m.p. 146–148 °C. ^1H NMR ($CDCl_3$, 400 MHz, 25 °C): δ = 11.43 (s, 1 H, OH), 7.28 (d, ^3J = 8.9 Hz, 2 H, 3-H, 5-H), 6.88 (d, ^3J = 8.9 Hz, 2 H, 2-H, 6-H), 3.78 (s, 3 H, OCH_3), 2.47 (s, 3 H, CH_3) ppm. ^{13}C NMR ($CDCl_3$, 75 MHz, 25 °C): δ = 197.5 (C=O), 159.9 (C-4), 155.4 (C=N), 131.0 (C-3, C-5), 121.0 (C-1 Ph), 113.2 (C-2, C-6), 55.2 (OCH_3), 26.2 (CH_3) ppm. IR (KBr): $\tilde{\nu}$ = 3235, 3186, 3018, 2961, 1663, 1610, 1519, 1435, 1362, 1298, 1258, 1179, 1024, 999, 950, 822, 729, 619 cm^{-1}. MS (FD): *m*/*z* (%) = 192.9 (100) $[M]^+$.

1-Hydroxyimino-1-(1-naphthyl)propan-2-one (14d): Compound **13d** (8.6 g, 46.7 mmol) was dissolved in diethyl ether (50 mL) and conc. hydrochloric acid (1 mL) was added. Isoamyl nitrite (6.6 g, 56.3 mmol) was added dropwise and the mixture heated at reflux for 2 h. After cooling (0 °C), the precipitate was collected, dissolved in NaOH (aq., 2.5 M), filtered, acidified with glacial acetic acid, cooled to 0 °C), and filtered. Recrystallization from toluene gave 7.1 g (33.3 mmol, 71%) of off-white crystals with m.p. 158–159 °C. ^1H NMR ($CDCl_3$, 400 MHz, 25 °C): δ = 11.67 (s, 1 H, OH), 7.86–

7.81 (m, 2 H, 4-H, 5-H), 7.51–7.47 (m, 1 H, 8-H), 7.45–7.37 (m, 3 H, 2-H, 3-H, 6-H), 7.24 (d, 1 H, 7-H), 2.60 (s, 3 H, CH_3) ppm. ^{13}C NMR ($CDCl_3$, 25 °C, 100 MHz): δ = 196.6 (C=O), 156.0 (C=N), 132.9, 130.2, 129.3, 128.7, 128.3, 126.6, 126.4, 126.0, 125.3, 26.1 (CH_3) ppm. IR (ATR): $\tilde{\nu}$ = 3368, 1671, 1388, 1358, 1300, 1258, 1225, 1160, 1091, 1021, 991, 937, 793, 773, 723 cm^{-1}. MS (FD): *m/z* (%) = 212.8 (100) $[M]^+$.

General Procedure for the Synthesis of 2,5-Dimethyl-3,6-diarylpyrazines 17 from Hydroxyimino Ketones 14: The 1-hydroxyimino-1-arylpropan-2-one **14** (1 equiv.) was dissolved in NaOH (5 N) and the solution added dropwise to a vigorously stirred suspension of zinc dust (4 equiv.) in aqueous NaOH (5 N) and toluene. The mixture was stirred for 2 h at 25 °C by external cooling. The organic layer was removed and replaced by pure toluene. After stirring for 1 h, the organic layer was separated, combined with the first toluene phase, and heated at reflux while bubbling air through the solution. The reaction was complete after 1 h (TLC), the toluene was removed in vacuo and the colorless residue recrystallized from CH_2Cl_2/methanol.

2,5-Dimethyl-3,6-diphenylpyrazine (17a): Yield: 38%, m.p. 125–126 °C (ref.[33] 126 °C). ^1H NMR ($CDCl_3$, 400 MHz, 25 °C): δ = 7.65–7.63 (m, 4 H, 2-H, 6-H Ph-p), 7.52–7.48 (m, 4 H, 3-H, 5-H Ph-p), 7.46–7.42 (m, 2 H, 4-H Ph-p), 2.65 (s, 6 H, CH_3) ppm. ^{13}C NMR ($CDCl_3$, 75 MHz, 25 °C): δ = 151.0 (C-2 Pz), 147.8 (C-1 Pz), 138.8 (C-1 Ph-p), 129.0 (C-2, C-6 Ph-p), 128.5 (C-3, C-5 Ph-p), 128.4 (C-4 Ph-p), 22.7 (CH_3) ppm. IR (ATR): $\tilde{\nu}$ = 3048, 1675, 1448, 1392, 1226, 1162, 1064, 1025, 963, 917, 795, 754, 695, 670 cm^{-1}. MS (FD): *m/z* (%) = 261.1 (100) $[M]^+$.

2,5-Dimethyl-3,6-bis(4-bromophenyl)pyrazine (17b): According to the general procedure, **14b** (19 g, 75.8 mmol), Zn (20.0 g, 0.31 mol), NaOH (150 mL), and toluene (100 mL) yielded 6.8 g (16.3 mmol, 42%) of a colorless solid with m.p. 220–222 °C. ^1H NMR ($CDCl_3$, 400 MHz, 25 °C): δ = 7.64 (d, ^3J = 8.4 Hz, 4 H, 2-H, 6-H Ph), 7.52 (d, ^3J = 8.4 Hz, 4 H, 3-H, 5-H Ph), 2.63 (s, 6 H, CH_3) ppm. ^{13}C NMR ($CDCl_3$, 100 MHz, 25 °C): δ = 150.1 (C-3, C-6 Pz), 147.8 (C-2, C-5 Pz), 137.4 (C-1 Ph), 131.6 (C-2, C-6 Ph), 130.7 (C-3, C-5 Ph), 123.1 (C-4 Ph), 22.6 (CH_3) ppm. IR (ATR): $\tilde{\nu}$ = 3021, 1441, 1396, 1384, 1160, 1073, 1007, 966, 827, 814, 715, 669 cm^{-1}. MS (FD): *m/z* (%) = 417.7 (100) $[M]^+$. $C_{18}H_{14}Br_2N_2$ (418.13): calcd. C 51.71, H 3.37, N 6.70; found C 51.17, H 3.38, N 6.67.

2,5-Dimethyl-3,6-bis(4-methoxyphenyl)pyrazine (17c): According to the general procedure, **14c** (3.6 g, 18.6 mmol), Zn (5.0 g, 76.5 mmol), NaOH (50 mL), and toluene (50 mL) yielded 0.7 g (12%) of a colorless solid with m.p. 189–191 °C. ^1H NMR ($CDCl_3$, 400 MHz, 25 °C): δ = 7.59 (d, ^3J = 8.8 Hz, 4 H, 2-H, 6-H Ph), 7.01 (d, ^3J = 8.8 Hz, 4 H, 3-H, 5-H Ph), 3.88 (s, 6 H, OCH_3), 2.64 (s, 6 H, CH_3) ppm. ^{13}C NMR ($CDCl_3$, 75 MHz, 25 °C): δ = 159.8 (C-4 Ph), 150.2 (C-3, C-6 Pz), 147.5 (C-2, C-5 Pz), 131.3 (C-1 Ph), 130.4 (C-2, C-6 Ph), 113.8 (C-3, C-5 Ph), 55.4 (OCH_3), 22.8 (CH_3) ppm. IR (KBr): $\tilde{\nu}$ = 2999, 2963, 2939, 1608, 1514, 1451, 1394, 1294, 1253, 1170, 1029, 835 cm^{-1}. MS (FD): *m/z* (%) = 320.0 (100) $[M]^+$. $C_{20}H_{20}N_2O_2$ (320.39): calcd. C 74.98, H 6.29, N 8.74; found C 74.58, H 6.14, N 8.64.

2,5-Dimethyl-3,6-di(1-naphthyl)pyrazine (17d): According to the general procedure, **14d** (6.0 g, 28.1 mmol), Zn (6.0 g, 91.8 mmol), NaOH (50 mL, 5 N), and toluene (50 mL) yielded 1.8 g (5.0 mmol, 36%) of a colorless solid with m.p. 240–241 °C. ^1H NMR ($CDCl_3$, 400 MHz, 25 °C): δ = 8.01–7.96 (m, 4 H, 2-H, 4-H Np), 7.67–7.60 (m, 6 H, 3-H, 5-H, 8-H Np), 7.28–7.51 (m, 4 H, 6-H, 7-H Np), 2.44 (s, 6 H, CH_3) ppm. ^{13}C NMR ($CDCl_3$, 75 MHz): δ = 151.6 (C-2 Pz), 149.5 (C-1 Pz), 136.2 (C-1 Np), 133.8 (C-8a Np), 131.3 (C-4a Np), 129.0 (C-4 Np), 128.5 (C-2 Np), 127.0 (C-8 Np), 126.6, 126.1, 125.4 (C-5, C-6, C-7 Np), 125.1 (C-3 Np), 21.9 (CH_3) ppm. IR (ATR): $\tilde{\nu}$ = 1507, 1404, 1369, 1154, 1124, 950, 800, 774, 732 cm^{-1}. MS (FD): *m/z* (%) = 359.9 (100) $[M]^+$. $C_{26}H_{20}N_2$ (360.45): calcd. C 86.64, H 5.59, N 7.77; found C 86.28, H 5.50, N 7.78.

2,5-Dimethyl-3,6-bis[4-(9-carbazolyl)phenyl]pyrazine (17e): CuI (20 mg, 0.11 mmol), copper powder (200 mg, 3.15 mmol), and K_2CO_3 (2.5 g, 18.1 mmol) were added to a solution of **14b** (3.0 g, 7.17 mmol) and carbazole (2.7 g, 15.8 mmol) in 1,2-dichlorobenzene (30 mL) and heated at 190 °C for 4 d. The mixture was cooled and diluted with $CHCl_3$, filtered, and concentrated in vacuo. The product was recrystallized from $CHCl_3$/toluene to yield 3.4 g (5.7 mmol, 80%) of an off-white solid with m.p. 324–326 °C. ^1H NMR ($CDCl_3$, 400 MHz, 25 °C): δ = 8.18 (d, ^3J = 7.6 Hz, 4 H, 4-H, 5-H Cb), 7.95 (d, ^3J = 8.4 Hz, 4 H, 2-H, 6-H Ph), 7.76 (d, ^3J = 8.4 Hz, 4 H, 3-H, 5-H Ph), 7.55 (d, ^3J = 8.2 Hz, 4 H, 1-H, 8-H Cb), 7.46 (t, 4 H, 2-H, 7-H Cb), 7.34 (t, 4 H, 3-H, 6-H Cb), 2.85 (s, 6 H, CH_3) ppm. IR (ATR): $\tilde{\nu}$ = 1603, 1518, 1448, 1392, 1220, 1167, 1069, 750, 739, 719, 676 cm^{-1}. MS (FD): *m/z* (%) = 294.2 (7) $[M]^{2+}$, 588.7 (100) $[M]^+$. $C_{42}H_{30}N_4$ (590.71): calcd. C 85.40, H 5.12, N 9.48; found C 84.98, H 5.03, N 9.13.

3,6-Diphenylpyrazine-2,5-dicarbaldehyde (19a): SeO_2 (382 mg, 3.44 mmol), **17a** (450 mg, 1.72 mmol) and 1,4-dioxane (0.3 mL) were added to diphenyl ether (25 mL). The mixture was heated at 180 °C and stirred for 4 d under nitrogen. The cooled mixture was filtered and purified by column chromatography on silica gel using gradient elution of diphenyl ether/petroleum ether changing to toluene/ethyl acetate (5:1). The product was recrystallized from toluene/petroleum ether, yield 280 mg (56%) of a yellow solid with m.p. 180 °C. R_f = 0.5 (toluene/ethyl acetate = 5:1). ^1H NMR ($CDCl_3$, 400 MHz, 25 °C): δ = 10.27 (s, 2 H, CHO), 7.80–7.78 (m, 4 H, 2-H, 6-H Ph-p), 7.59–7.57 (m, 6 H, 3-H, 4-H, 5-H Ph-p) ppm. ^{13}C NMR ($CDCl_3$, 75 MHz, 25 °C): δ = 190.2 (CHO), 153.0 (C-1 pyr), 143.9 (C-2 pyr), 134.3 (C-1 Ph-p), 130.7 (C-2, C-6 Ph-p), 130.1 (C-3, C-5 Ph-p), 128.8 (C-4 Ph-p) ppm. IR (KBr): $\tilde{\nu}$ = 3056, 2873, 1704, 1448, 1421, 1353, 1200, 1170, 1081, 1065, 1023, 847, 769, 702 cm^{-1}. MS (FD): *m/z* (%) = 288.2 (100) $[M]^+$. HRMS: calcd. $C_{18}H_{12}O_2N_2Na$ 311.0800; found 311.0797.

3,6-Bis(4-methoxyphenyl)pyrazine-2,5-dicarbaldehyde (19c): Prepared from **17c** according to the procedure for **19a**, yield 100 mg (21%) of an orange solid with m.p. 167 °C. ^1H NMR ($CDCl_3$, 300 MHz): δ = 10.24 (s, 2 H, CHO), 7.78 (d, ^3J = 8.8 Hz, 4 H, 2-H, 6-H ph), 7.08 (d, ^3J = 8.8 Hz, 4 H, 3-H, 5-H, ph), 3.93 (s, 6 H, OCH_3) ppm. ^{13}C NMR ($CDCl_3$, 75 MHz): δ = 190.6 (CHO), 161.9 (C4 ph), 151.8 (C2, C5 pz), 143.2 (C3, C6 pz), 131.7 (C1 ph), 126.7 (C2, C-6 ph), 114.4 (C3, C-5 ph), 55.5 (OCH_3) ppm. IR (KBr): $\tilde{\nu}$ = 2932, 2841, 1706, 1606, 1518, 1417, 1255, 1176, 1026, 840 cm^{-1}. MS (FD): *m/z* (%) = 348.2 (100) $[M]^+$. HRMS: calcd. for $C_{20}H_{17}O_4N_2$ 349.1189; found 349.1193.

Supporting Information (see footnote on the first page of this article): ^1H and ^{13}C NMR spectra and UV/Vis/fluorescence spectra of compounds **1**–**12**.

Acknowledgments

The authors thank the Deutsche Forschungsgemeinschaft (DFG) for financial support, H. Kolshorn for NMR spectra, and the referees of this article for important advice.

[1] a) W. Tachelet, S. Jacobs, H. Ndayikengurukiye, H. J. Geise, J. Gruner, *Appl. Phys. Lett.* **1994**, *64*, 2364–2366; b) Y. D. Jin,

H. Z. Chen, P. L. Heremans, K. Aleksandrzak, H. J. Geise, M. van der Auweraer, *Synth. Met.* **2002**, *127*, 155–158; c) U. Stalmach, H. Detert, H. Meier, V. Gebhardt, D. Haarer, *Optical Mater.* **1998**, *9*, 77–81; d) J. P. Yang, P. L. Heremans, R. Hoefnagels, P. Dieltiens, F. Blockhuys, H. J. Geise, G. Borghs, *Synth. Met.* **2000**, *108*, 95–100; e) U. Scherf, *Top. Curr. Chem.* **1999**, *201*, 163–222.

[2] a) D. S. Chemla, *Nonlinear optical properties of organic molecules and crystals*, Academic Press, Boston, MA, **1987**; b) B. Strehmel, A. M. Sarker, H. Detert, *ChemPhysChem* **2003**, *4*, 249–259; c) S. J. K. Pond, O. Tsutsumi, M. Rumi, O. Kwon, E. Zojer, J. L. Brédas, S. R. Marder, J. W. Perry, *J. Am. Chem. Soc.* **2004**, *126*, 9291–9306; d) B. Lange, R. Zentel, C. Ober, S. Marder, *Chem. Mater.* **2004**, *16*, 5286–5292.

[3] a) J. Tolosa, J. J. Bryant, K. M. Soltsnev, K. Brödner, L. M. Tolbert, U. H. F. Bunz, *Chem. Eur. J.* **2011**, *17*, 13726–13731; b) G. Grynkiewicz, M. Poenie, R. Y. Tsien, *J. Biol. Chem.* **1985**, *260*, 3440–3450; c) A. Zucchero, J. Tolosa, L. M. Tolbert, U. H. F. Bunz, *Chem. Eur. J.* **2009**, *15*, 13075–13081.

[4] a) H. Meier, U. Stalmach, H. Kolshorn, *Acta Polymer* **1997**, *48*, 379–384; b) J. Gierschner, J. Cornil, H.-J. Egelhaaf, *Adv. Mater.* **2007**, *19*, 173–191.

[5] a) V. Schmitt, S. Glang, J. Preis, H. Detert, *Sens. Lett.* **2008**, *6*, 1–7; b) H. Detert, V. Schmitt, *J. Phys. Org. Chem.* **2006**, *19*, 603–607; c) H. Detert, V. Schmitt, *J. Phys. Org. Chem.* **2004**, *17*, 1051–1057; d) T. Verbiest, S. Houbrechts, M. Kauranen, K. Clays, A. Persoons, *J. Mater. Chem.* **1997**, *7*, 2175–2189; e) D. Schollmeyer, H. Detert, *Acta Crystallogr., Sect. E* **2011**, *67*, o1384–o1385; f) V. Schmitt, S. Glang, H. Detert, *Adv. Sci. Technol.* **2010**, *75*, 103–107; g) C. Wang, T. Zhang, W. Lin, *Chem. Rev.* **2012**, *112*, 1084–1104.

[6] a) J. Kumpf, U. H. F. Bunz, *Chem. Eur. J.* **2012**, *18*, 8921–8924; b) V. Schmitt, S. Glang, J. Preis, H. Detert, *Adv. Sci. Technol.* **2008**, *55*, 36–41.

[7] a) A. Alder, B. Steven, J. Berger, N. Blom, M. Marizel, *Optical Sensor system for determining pH values and Ionic strength*, WO 1995030148 A1, **1995**; b) G. J. Mohr, O. S. Wolfbeiß, *Anal. Chim. Acta* **1995**, *316*, 239–246; c) S. A. Hilderbrand, R. Weissleder, *Tetrahedron Lett.* **2007**, *48*, 4383–4385; d) D. P. Flaherty, T. Kiyota, Y. X. Dong, T. Ikezu, J. L. Vennerstrom, *J. Med. Chem.* **2010**, *53*, 7992–7999; e) S. Yan, R. Huang, Y. Zhou, M. Zhang, M. Deng, X. Wang, X. Wenig, X. Zhou, *Chem. Commun.* **2011**, *47*, 1273–1275.

[8] a) S. Petrova, Y. Kostov, K. Jeffris, G. Rao, *Anal. Lett.* **2007**, *40*, 715–727; b) H. Sunahara, Y. Urano, H. Kojima, T. Nagano, *J. Am. Chem. Soc.* **2007**, *129*, 5597–5609; c) Y.-L. Zhang, J. A. Frangos, M. Chachisvilis, *Biochem. Biophys. Res. Commun.* **2006**, *347*, 838–841.

[9] G. S. He, L. Yuan, Y. Cui, M. Li, P. N. Prasad, *J. Appl. Phys.* **1997**, *81*, 2529–2537.

[10] a) R. G. Selsby, P. Pennance, K. I. Barnhard, *J. Quant. Chem.* **1990**, *37*, 539–546; b) R. Cristiano, E. Westphal, I. H. Bechtold, A. J. Bortoluzzi, H. Gallardo, *Tetrahedron* **2007**, *63*, 2851–2858; c) S. Achelle, Y. Ramondenc, G. Dupas, N. Plé, *Tetrahedron* **2008**, *64*, 2783–2791; d) L. Pascal, J. J. Vanden Eynde, Y. Van Haverbeke, P. Dubois, A. Michel, U. Rant, E. Zojer, G. Leising, L. O. Van Dorn, N. E. Gruhn, J. Cornil, J.-L. Brédas, *J. Phys. Chem. B* **2002**, *106*, 6442–6450; e) S. Achelle, I. Nouira, B. Pfaffinger, Y. Ramondenc, N. Plé, J. Rodríguez-López, *J. Org. Chem.* **2009**, *74*, 3711–3717.

[11] a) J. N. Wilson, U. H. F. Bunz, *J. Am. Chem. Soc.* **2005**, *127*, 4124–4125; b) H. Detert, E. Sugiono, *J. Lumin.* **2005**, *112*, 372–376; c) H. Detert, E. Sugiono, *Synth. Met.* **2004**, *147*, 233–236.

[12] a) H. Lindauer, P. Czerney, U.-W. Grummt, *J. Prakt. Chem.* **1994**, *336*, 521–524; b) C. J. Kelley, K. Ansu, W. Budisosetyo, A. Ghiorgis, Y. Qin, J. M. Kauffman, *J. Heterocycl. Chem.* **2001**, *38*, 11–23; c) C. Lambert, S. Stadler, G. Bourhill, C. Bräuchle, *Angew. Chem.* **1996**, *108*, 710–712; *Angew. Chem. Int. Ed. Engl.* **1996**, *35*, 644–646.

[13] a) H. I. X. Mager, W. Berends, *Rec. Trav. Chim. Pays-Bas* **1958**, *77*, 827–841; b) L. Scaccianoce, N. Feeder, S. Teat, E. A. Marseglia, A. C. Grimsdale, A. B. Holmes, *Acta Crystallogr., Sect. C* **2000**, *56*, 1277–1279; c) S.-Y. An, S.-D. Xu, Q.-D. Zeng, Z.-Y. Tan, C. Wang, L.-J. Wan, C.-L. Bai, *Wuli Huaxue Xuebao* **2005**, *21*, 925–928 (*Chem. Abstr.*, **2005**, *144*, 75336).

[14] a) S. M. Al-Hazmy, A. S. Babaqi, E. Daltrozzo, M. Klink, J. Sauter, E. M. Ebeid, *J. Photochem. Photobiol. B: Biology* **1999**, *122*, 17–22; b) S. A. El-Daly, E. Z. M. Ebeid, S. M. El-Hazmy, A. S. Babaqi, Z. El-Gohary, G. Duportail, *Proc. Indian Acad. Sci. Chem. Sci.* **1993**, *105*, 651–658; c) Z. Li, S. Wu, *J. Fluoresc.* **1997**, *7*, 237–242; d) J. C. Collette, A. W. Harper, *Proc. SPIE* **2003**, 184–192; e) V. Schmitt, J. Fischer, H. Detert *ISRN Organic Chemistry* **2011**, DOI: 10.5402/2011/589012; f) N. A. Nemkovich, H. Detert, A. N. Sobchuk, *J. Appl. Spectrosc.* **2012**, *78*, 787–793.

[15] a) F. Guo, J. Marti-Rujas, Z. Pan, C. E. Hughes, K. D. M. Harris, *J. Phys. Chem. C* **2008**, *112*, 19793–19796; b) A. Collas, I. Bagrowska, K. Aleksandrzak, M. Zeller, F. Blockhuys, *Cryst. Growth Des.* **2011**, *11*, 1299–1309; c) J. Fischer, V. Schmitt, D. Schollmeyer, H. Detert, *Acta Crystallogr., Sect. E* **2011**, *67*, o875.

[16] a) H. H. Perkampus, Th. Bluhm, *Tetrahedron* **1972**, *28*, 2099–2110; b) T. Teshirogi, *Jpn. Kokai Tokkyo Koho*, JP 01113375 A, **1989** (*Chem. Abstr.* **1989**, *111*, 233858).

[17] a) A. E. Siegrist, *Helv. Chim. Acta* **1967**, *50*, 906–957; b) A. E. Siegrist, H. R. Meyer, P. Gassmann, S. Moss, *Helv. Chim. Acta* **1980**, *63*, 1311–1134.

[18] J. J. Vanden Eynde, L. Pascal, Y. Van Haverbeke, P. Dubois, *Synth. Commun.* **2001**, *31*, 3167–3173.

[19] a) J. Schoenhaber, W. Frank, T. J. J. Mueller, *Org. Lett.* **2010**, *12*, 4122–4125; b) J.-Y. Jaung, *Dyes Pigm.* **2006**, *71*, 245–250; c) P. Czerney, U.-W. Grummt, *Sens. Actuators B* **1997**, *39*, 395–400; d) P. Singh, A. Baheti, K. R. J. Thomas, *J. Org. Chem.* **2011**, *76*, 6134–6145; e) S. Achelle, A. Barsella, C. Baudequin, B. Caro, F. Robin-le Guen, *J. Org. Chem.* **2012**, *77*, 4087–4096.

[20] R. Bartnik, R. Faure, K. Gebicki, *Acta Crystallogr., Sect. C* **1999**, *55*, 1034–1037.

[21] a) J. Fischer, V. Schmitt, D. Schollmeyer, H. Detert, *Acta Crystallogr., Sect. E* **2011**, *67*, o875; b) V. Schmitt, D. Schollmeyer, H. Detert, *Acta Crystallogr., Sect. E* **2011**, *67*, o1553.

[22] Calculations: MOPAC package, WinMOPACV2.0, Fujitsu ; optimized geometries were obtained at the AM1 level, excited states by INDO/S.

[23] P. Suppan, N. Ghoneim, *Solvatochromism*, Royal Society of Chemistry, Cambridge, UK, **1997**, p. 17.

[24] N. A. Nemkovich, H. Detert, V. Schmitt, *Chem. Phys.* **2010**, *378*, 37–41.

[25] a) C. E. M. Carvalho, I. M. Brinn, A. V. Pinto, M. d. C. F. R. Pinto, *J. Photochem. Photobiol. A: Chem.* **2000**, *136*, 25–33; b) F. Terenziani, A. Painelli, C. Katan, M. Charlot, M. Blanchard-Desce, *J. Am. Chem. Soc.* **2006**; *128*, 15742–15755.

[26] a) C. Reichardt, *Solvents and Solvent Effects in Organic Chemistry*, Wiley-VCH, Weinheim, Germany, **2003**; b) J. Catalán, J. L. G. de Paz, C. Reichardt, *J. Phys. Chem. A* **2010**; *114*, 6226–6234; c) J. Catalán, C. Reichardt, *J. Phys. Chem. A* **2012**, *116*, 4726–4734.

[27] C. Wink, H. Detert, *J. Phys. Org. Chem.* **2013**, *26*, 137–143.

[28] Further information, wavenumbers and standard errors are listed in the Supporting Information.

[29] J. Catalán, *J. Phys. Chem. B* **2009**, *113*, 5951–5960.

[30] R. S. Becker, *Theory and interpretation of fluorescence and phosphorescence*, Wiley, New York, **1969**.

[31] a) E. Lippert, *Z. Elektrochem.* **1957**, *61*, 695; b) W. Baumann, H. Deckers, K.-D. Losen, F. Petzke, *Ber. Bunsen-Ges.* **1977**, *81*, 799; c) N. Mataga, Y. Kaifu, M. Koizumi, *Bull. Chem. Soc. Jpn.* **1956**, *29*, 465.

[32] W. Liptay, *Die Lösungsmittelabhängigkeit der Wellenzahl von Elektronenbanden und die chemisch-physikalischen Grundlagen*,

in: *Optische Anregung organischer Systeme* (Ed.: W. Foerst), Verlag Chemie, Weinheim, Germany, **1966**, p. 263–339.
[33] Z. Li, S. Wu, *J. Fluoresc.* **1997**, *7*, 237–242.
[34] W. Liptay, R. Wortmann, R. Böhm, N. Detzer, *Chem. Phys.* **1988**, *120*, 439–448.
[35] D. M. Togashi, S. M. B. Costa, A. J. F. N. Sobral, A. M. d'A. R. Gonsalves, *Chem. Phys.* **2004**, *300*, 267–275.
[36] a) H. G. O. Becker, *Einführung in die Photochemie*, 2nd ed., Thieme, Stuttgart, Germany, **1983**; b) Th. Förster, *Z. Elektrochem.* **1950**, *54*, 42–45.
[37] T. Eicher, S. Hauptmann, in: *Chemie der Heterocyclen*, Thieme, Stuttgart, Germany, **1994**.
[38] J. R. Lackowicz, *Principles of Fluorescence Spectroscopy*, 2nd ed., Kluwer, New York, **1999**, p. 57.
[39] A. Najafi, *J. Labelled Compd. Radiopharm.* **1987**, *10*, 1167–1175.
[40] K. Jozwiak, C. Khalid, M. J. Tanga, I. Berzetei-Gurske, L. Jimenez, J. A. Kozocas, A. Woo, W. Zhu, R.-P. Xiao, D. R. Abernethy, I. W. Wainer, *J. Med. Chem.* **2007**, *50*, 2903–2915.
[41] a) W. Borsche, *Chem. Ber.* **1907**, *40*, 737–744; b) W. F. Breech, *J. Chem. Soc.* **1955**, 3094–3098.
[42] C. Weygand, R. Gabler, *J. Prakt. Chem.* **1940**, *155*, 332–340.
[43] J. C. Duff, V. I. Furness, *J. Chem. Soc.* **1952**, 1159–1164.
[44] a) J. Lewis, J. Moore, *Dalton Trans.* **2004**, *9*, 1376–1385; b) J. P. Dix, F. Vögtle, *Chem. Ber.* **1980**, *113*, 457–470.
[45] R. Brettle, D. A. Dunmur, N. J. Hindley, C. M. Marson, *J. Chem. Soc. Perkin Trans. 1* **1993**, 775–782.
[46] W. Stilz, H. Pommer, K. H. Koenig (BASF), DE 1112072, **1959** (*Chem. Abstr.* **1962**, *56*, 2378).
[47] V. Jagodic, B. Bozic, Lj. Tusek-Bozic, M. J. Herak, *J. Heterocycl. Chem.* **1980**, *17*, 685–688.
[48] G. M. Sheldrick, *SHELXL97, Program for Crystal Structure Refinement*, University of Göttingen, Germany, **1997**.

Received: March 30, 2013
Published Online: ■

